Progress in Oceanography
December 2023, Volume 219 Pages 103154 (20p.)
https://doi.org/10.1016/j.pocean.2023.103154
https://archimer.ifremer.fr/doc/00859/97082/

Unravelling mechanisms behind population dynamics, biological traits and latitudinal distribution in two benthic ecosystem engineers: A modelling approach

De Cubber Lola [1, 2, *], Lefebvre Sebastien [1], Lancelot Theo [1], Schaffer Ferreira Jorge Daniel [1], Gaudron Sylvie Marylène [1, 3]

[1] Univ. Lille, Univ. Littoral Côte d'Opale, CNRS, IRD, UMR 8187 Laboratoire d'Océanologie et de Géosciences, F-59000 Lille, France
[2] MARBEC, Univ Montpellier, CNRS, IFREMER, IRD, Sète, France
[3] Sorbonne Univ., UFR 918, 75005 Paris, France

* Corresponding author : Lola De Cubber, email address : lola.decubber@gmail.com

sebastien.lefebvre@univ-lille.fr ; theo.lancelot@gmail.com ; daniel.jorge@univ-littoral.fr ; sylvie.gaudron@upmc.fr

Abstract :

The mechanistic approach consisting of coupling Dynamic Energy Budget (DEB) models to Individual-Based Models (IBMs) allows simulating individual and population biological traits and their dynamics. This approach was developed here to study population dynamics of two sympatric intertidal ecosystem engineers, Arenicola marina and Arenicola defodiens (Annelida Polychaeta) occurring in the North-East Atlantic from Portugal to Sweden. Latitudinal heterogeneity of the two species' performances were investigated in terms of population dynamics and biological traits using latitudinal differences in environmental forcing variables. The impact of the forcing variables on population dynamics processes (shore colonisation and migration, spawning and recruitment, etc.) within a specific foreshore (mean values and seasonal patterns) was also assessed. Published DEB parameters were used for A. marina and a specific calibration was undertaken for A. defodiens, combining literature data and new laboratory experiments and field data. Our DEB-IBM simulated super-individuals' growth and reproduction while lugworms were colonising, migrating and dying over a simulated foreshore. Density rules affected population dynamics. Environmental forcings consisted in monthly values of chlorophyll-a (chl-a) concentrations and daily values of SST. Scenarios focusing on the two most contrasted of these forcing variables time series were used to explore their relative effects over populations' dynamics and on-shore processes were investigated at two sites displaying highly different simulated population abundances. Overall, northern sites with higher chl-a levels performed better displaying higher biomass, maximum length and reproductive outputs for both species. As expected, Sea Surface Temperature (SST) changes between sites did not impact greatly populations dynamics. Under favourable environmental conditions, intra- and inter-specific competitions emerged from the model. Under non-favourable environmental conditions, A. defodiens' populations crashed and A. marina displayed atypical population processes, with rare spawning events barely allowing the population's renewal, and lower size at maturity. Further use and development of this model will lead to better insights on the lugworm populations' evolution over the next decades.

Graphical abstract

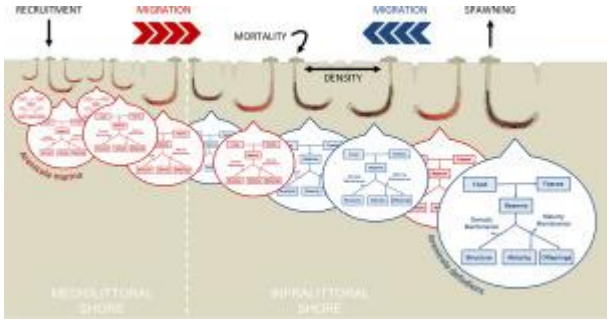

Graphical representation of the DEB-IBM developed in this study. Individuals from two species of lugworms displaying different shore colonisation patterns are followed. Their length, reproduction rate and development are obtained from DEB models, and other population processes are considered (e.g. mortality, predation) on a simulated shore where density is a limiting factor.

Highlights

► A Dynamic Energy Budget - Individual-Based Model was developed for two benthic polychaetes. ► Population dynamics were simulated under environmental condition recovered from Portugal to Sweden. ► Northern sites with higher chl-a levels performed better (higher biomass and maximum length). ► Under favourable conditions, intra- and inter-specific competition emerged from the model. ► Under non-favourable conditions, *A. defodiens*' populations crashed.

Keywords : Dynamic Energy Budget model, Individual-Based model, Arenicola marina, Arenicola defodiens, North-east atlantic

1. Introduction

Coastal ecosystems are subject to many and intensifying anthropogenic pressures (Halpern et al., 2015) and therefore require a better understanding of their functioning and biodiversity dynamics, which is becoming a growing challenge for marine ecologists (Mangano et al., 2020; Thomas and Bacher, 2018; Harley et al., 2006). In the context of global change, correlative niche models linking population dynamics processes such as survival or reproduction rates to a set of environmental variables might lead to poor predictive power when transferred to novel environments (Davis et al., 1998). As a consequence, a number of population dynamics approaches have been developed in order to explain and predict how biodiversity reacts to the environmental variability or to anthropogenic pressures (Batabyal, 1996; Caswell, 2001; Coulson, 2012; Grimm, 1999; Holmes et al., 1994; Huston et al., 1988; Picard and Liang, 2014). Overall, these models consist in studying the changes in numbers and size or age-structure of a population through time and space of a single species or more rarely of several species populations occurring as a consequence of population level processes including death (natural death or linked to predation, disease or harvesting) and the arrival of new individuals (via larval dispersal or migration, Wethey et al., 2011). However, these models are generally based on statistical correlations and not on a mechanistic understanding of the individual (physiological and behavioural) and population processes (inter-individual variability, dispersal and migrations) at stake (Kearney et al, 2010).

In order to address this issue, mechanistic models based on the knowledge of the physiological, phenological, behavioural or other responses of organisms to environmental variables have been developed (Malishev et al., 2017; Thomas and Bacher, 2018; Martin et al., 2012). They constitute promising tools for predicting species responses to climate change and understanding the mechanisms behind those responses. Among these approaches, Dynamic Energy Budget (DEB) models have been associated to Individual Based Models (IBM) to predict population dynamics and address an variety of ecological questions ranging from ecotoxicology (David et al., 2019; Beaudouin et al., 2012), fish ecology and fisheries management (Haberle et al., 2023), aquaculture (Bacher and Gangnery, 2006), and the study of potential impacts of climate change (Thomas and Bacher, 2018; Thomas et al., 2020). Dynamic Energy Budget (DEB) models simulate the effect of changing environmental conditions on the individuals' bioenergetics by quantifying the energy allocation to reserve, growth, maturation, reproduction and maintenance of a species at the individual level throughout its life cycle, thus providing predictions of growth, reproduction and life-history traits of individuals according to environmental conditions such as temperature and food availability (Kooijman, 2010). Over the last 25 years, the theory has kept expanding and models based on the DEB theory have been applied to over 3000 species with a wide variety of applications (https://www.bio.vu.nl/thb/deb/deblab/add_my_pet/). Combined with agent-based or IBMs that focus on individual processes in order to understand higher levels of biological complexity such as population dynamics (De Angelis and Grim, 2014), they enable estimating

the impact of varying environmental conditions not only at the individual level but also at the population level (Kearney et al., 2009; 2010; Malishev et al., 2017; Thomas and Bacher, 2018). In practice, single individuals can be followed, or populations are divided into a number of cohorts followed as discrete entities. In the latter case, cohorts are treated individually as super-individuals with the same DEB state variables. Each super-individual can contain all individuals from a given age cohort, integrating inter-individual variability, or a given number of individuals with the same properties and no inter-individual variability. New cohorts can be generated depending on the reproductive status of the followed cohorts (Pethybridge et al., 2013; Thomas and Bacher, 2018). Functional traits can then be extracted from the obtained population dynamics (Mangano et al, 2019). Functional traits are "morphological, biochemical, physiological, structural, phenological, or behavioural characteristics of organisms that influence how they respond to the environment (response traits) and/or their effects on ecosystem properties (effect traits)" (Violle et al., 2007). The comparison of response traits (for example biomass or reproductive output) can help identifying optimal environmental conditions for a given species and scenario-specific quantitative maps of biomass or reproductive output can then be considered to inform fisheries management (Mangano et al., 2019). As an example, the identification of areas with predicted high abundance can help defining protection areas (Mangano et al., 2020). The most common biological population response traits generally used are linked with population and individual growth (abundance, biomass and maximum length of individuals) and reproduction (total reproductive output and length at first maturity) (Mangano et al, 2020).

Here, we used DEB-IBM to study the population dynamics and biological traits of two widespread engineer species, the lugworm *Arenicola marina* (Linnaeus, 1758) and the black lugworm *Arenicola defodiens* (Cadman and Nelson-Smith, 1993) along the North-East Atlantic coast. Among the species diversity within ecosystems, engineer species possess functional traits that largely and non-linearly influence their surrounding environment, providing key ecosystem functions and services such as nutrient recycling or ecosystem resilience and stability (see Yeakel et al., 2020; Wrede et al., 2019). *A. marina* and *A. defodiens* are psammivarous benthic polychaetes (Annelida) inhabiting sandy shores on the Eastern Atlantic coast from Portugal to the Arctic (Pires et al., 2015; Volkenborn, 2005). Both species live within galleries dug in the sediment up to 30 to 40 cm deep for *A. marina* and up to 70 cm deep for *A. defodiens*. They ingest the superficial (for *A. marina*) or deeper (for *A. defodiens*) sediment to feed on the organic matter it contains, and create a water current bringing oxygen to their gills and tegument (Cadman and Nelson-Smith, 1993; Senga Green et al., 2016). This bioturbation modifies the abiotic conditions within the sediment (grain size, nitrogen and oxygen content) and impacts the associated communities' composition, enhancing selected species at the expense of others (Clarke et al., 2017; Kristensen, 2001; Reise, 1985; Volkenborn, 2005). Records of their shore distribution showed that they can live separately occupying different bathymetric levels on the same shore or in sympatry on the same bathymetric level

(Cadman, 1997; De Cubber et al, 2018). Apart from their ecological role, the species are still used as baits and commonly harvested in Europe (UK, France, the Netherlands, etc.) by professional and recreational fishermen (Watson et al., 2017). Over-exploitation of these species has long been feared and reported (Blake, 1979; Olive, 1993) and confirmed recently in some areas (De Cubber et al., 2018), potentially leading to changes in size and age structure, abundance and distribution of local populations. Conversely, in Southern Europe, their expansion has been reported locally and might impact other native species with high ecological value such as the eelgrass, *Zostera noltii* (Pires et al., 2015). Our interest was thus to be able to simulate population dynamics at both a small local (foreshore scale) and a wide (North-East Atlantic coast) scale to then be able to address the questions around the local differences of shore distribution, the local impacts of harvesting on single shores and the possible environmental change effects on overall latitudinal distributions.

Physiology and behaviour of the two species have been studied unevenly. *A. marina* individual responses to different environmental conditions have already been simulated with a Dynamic Energy Budget model (De Cubber et al., 2019; 2020). The study showed that Sea-Surface Temperature (SST) and planktonic Chlorophyll-a concentration (chl-a) are relevant forcing variables to properly simulate the species response to environment (De Cubber et al., 2020). The down-shore migration of *A. marina* individuals while growing has also already been documented (De Cubber et al., 2020), and the future distribution trends investigated with age-structured meta-population models considering varying mortality rates according to heat waves (Wethey and Woodin, 2022). Nevertheless, no study representing expressively the mechanisms influencing the species dynamics and survival were developed until now to our knowledge. *A. defodiens* was much less studied and few data are available regarding the species individual and population traits, and hence the potential interaction (in terms of spatial competition) between both species.

We used spatially explicit forcing variables to drive DEB models at the individual scale to simulate the life-history traits at the population scale of two lugworm's species, *A. marina* and *A. defodiens* (i.e. growth and reproduction) as a function of environmental variables (i.e. SST and chl-a). We then integrated each DEB model into a individual-based density-dependent population dynamic model (DEB-IBM, Martin et al., 2012) and applied the DEB-IBM to a number of locations in Europe where the two polychaetes species have been already studied on a latitudinal gradient during the period 2010-2020. Our main objectives were:

1. To develop a two-species DEB-IBM reflecting the most comprehensive way processes involved into the species population dynamics, namely: the generation of new individuals (or super individuals) based on reproduction, the variability of some model parameters, the mobility and habitat preferences of the individuals and mortality;

2. To simulate potential latitudinal discrepancies between lugworm populations in terms of population dynamics and biological traits (length at puberty, maximum body size, size distribution, biomass, abundance and total reproductive output) explained by latitudinal differences

in environmental forcings;

3. To understand the impact of the two forcing factors (temperature and chl-a) on population dynamics processes (shore colonisation and migration, spawning and recruitment, etc.) of the two lugworm species within a specific foreshore (mean values, inter-annual and seasonal patterns).

2. Material and Methods

2.1. Dynamic Energy Budget Models

2.1.1. Description

DEB models and lifecycle. The DEB theory describes the energy flows within an organism between three compartments (state variables): the reserve (E), the structure (V), and the maturity (E_H) or the reproduction buffer (offsprings) (E_R) according to its life stage in order to describe its energy allocation to growth, reproduction and maintenance for a given food level and at a reference temperature T_{ref} (Kooijman, 2010). The DEB model equations for *A. marina* and the link between the model and the species' lifecycle have already been described by De Cubber et al. (2019; 2020) (see Table 1).

Briefly, both lugworm species exhibit annual iteroparity (Watson et al., 2000). Populations of *A. marina* have been reported to spawn epidemically over a few days to two weeks from September to November depending on the targeted populations (Luttikhuizen and Dekker, 2010; Howie, 1984; Watson et al., 2000). After spawning, non-feeding trochophore larvae of *A. marina* disperse to a subtidal temporary habitat where they start feeding on deposited and suspended particles and experience a metabolic acceleration (e.g the acceleration of all metabolic rates, see Kooijman, 2014) until the end of metamorphosis. After metamorphosis, the post-larval stages (juvenile stage) will disperse again in the water column and recruit on the high mediolittoral sandy foreshores, acquiring the psammivorous feeding behaviour of adults in spring to early summer. At this point, metabolic acceleration ceases and juveniles will gradually migrate lower on the shore and reach sexual maturation (puberty stage) (Sup. Mat. 1, De Cubber et al., 2019). Given the really close phylogenetic relationship between *A. marina* and *A. defodiens*, the same abj-DEB model (accounting for metabolic acceleration between the first feeding and the end of metamorphosis) was used for both species with two different sets of parameters (see De Cubber et al., 2019; 2020). The lifecycle of *A. defodiens* in a natural environment has barely been described, except for spawning events that have been reported from mid-December to early January (De Cubber et al., 2018; Watson et al., 1998). However, based on *in situ* pers. observations (the authors and M. Crouvoisier), we have made the hypothesis that individuals of *A. defodiens* disperse and recruit in subtidal muddy habitats, and gradually reach infralittoral soft bottoms when reaching their sexual maturity (see Sup. Mat. 1).

Table 1: Summary of the mathematical expressions used to build the Dynamic Energy Budget Individual-Based model (see Kooijman, 2010; De Cubber et al., 2020 for further details on the DEB models for *A. marina* and *A. defodiens*). DEB and IBM parameters are detailed in Table 2. L is the structural length (cm) with $L = V^{1/3}$, and L_b and L_j are the structural lengths at birth and metamorphosis respectively. a_j is the age at metamorphosis. TTR is the temperature tolerance range of the species. GSI is the wet weight of gametes divided by the total wet weight and GSI_{trigger} the GSI leading to spawning. x_i is the shore level of individual i and x_{subtidal} the shore level assigned to subtidal environment. d_x and $d_{max,x}$ are respectively the density at x and the maximum possible density at x. *bath* is the bathymetry theoretically occupied by a lugworm according to its trunk length TL_w (De Cubber et al., 2020). $Capacity_{\text{shore}}$ is the shore capacity in terms of abundance of lugworms, calculated according the max density per shore level. $N_{\text{Offspring,emitted},i}$ is the number of offspring spawned per female, among which a (reduced) number $N_{\text{Offspring,shore},i}$ offspring are simulated. RO_i is the reproductive output of individual i. Wx stands for Wimereux (East English Channel, France).

Dynamic Energy Budget Model equations		
State variables	Reserve	$\frac{dE}{dt} = \dot{p}_A - \dot{p}_C$
	Structure	$\frac{dV}{dt} = \frac{\dot{p}_G}{[E_G]}$
	Maturity	if $E_H < E_H^p$ $\frac{dE_H}{dt} = \dot{p}_H$; else $\frac{dE_H}{dt} = 0$
	Reproduction	if $E_H \geqslant E_H^p$, $\frac{dE_R}{dt} = \kappa_R \cdot \dot{p}_R$; else $\frac{dE_R}{dt} = 0$
Fluxes	Ingestion	$\dot{p}_X = \frac{\dot{p}_A}{\kappa_X}$
	Assimilation	$\dot{p}_A = \{\dot{p}_{Am}\} \cdot s_M \cdot f \cdot V^{2/3}$
	Mobilisation	$\dot{p}_C = E \cdot \frac{\dot{v} \cdot s_M \cdot V^{2/3} \cdot [E_G] + \dot{p}_S}{\kappa \cdot E + V \cdot [E_G]}$
	Somatic maintenance	$\dot{p}_S = [\dot{p}_M] \cdot V$
	Maturity maintenance	$\dot{p}_J = \dot{k}_J \cdot E_H$
	Growth	$\dot{p}_G = \kappa \cdot \dot{p}_C - \dot{p}_S$
	Reproduction	$\dot{p}_R = (1-\kappa) \cdot \dot{p}_C - \dot{p}_J$
	Maturity	$\dot{p}_H = (1-\kappa) \cdot \dot{p}_C - \dot{p}_J$
Metric relationships	Physical length (cm)	$L_w(t) = \frac{V(t)^{1/3}}{\delta}$
	Wet weight (g)	$W_w(t) = d_V \cdot V(t) + (E(t) + E_R(t)) \cdot \frac{w_{Ed} \cdot d_E}{\mu_{Ed} \cdot d_{Ed}}$
Reproduction buffer handling rules	*A. marina*	if ($\Delta SST_{14} \geqslant 1$ °C and $GSI \geqslant 0.1.W_w = GSI_{\text{trigger}}.W_w$), spawn (set $E_R = 0$)
	A. defodiens	if ($day = 15^{th} of December$), spawn (set $E_R = 0$)
Acceleration coefficient	if $E_H < E_H^b$ $s_M = 1$; if $E_H^b \leqslant E_H < E_H^j$ $s_M = L/L_b$; else $s_M = L_j/L_b$ if $E_H \geqslant E_H^j$	
Shape coefficient	if $E_H < E_H^b$ $\delta = \delta_{Me}$; if $E_H^b \leqslant E_H < E_H^j$ $\delta = \delta_{Me} + (\delta_M - \delta_{Me}) \cdot (\frac{L - L_b}{L_j - L_b})$; else $\delta = \delta_M$ if $E_H \geqslant E_H^j$	
Arrhenius temperature	$\dot{k}(T) = \dot{k}_1 \cdot \exp\left(\frac{T_A}{T_{ref}} - \frac{T_A}{T}\right) \cdot \frac{1 + \exp\left(\frac{T_{AL}}{T_{ref}} - \frac{T_{AL}}{T_L}\right) + \exp\left(\frac{T_{AH}}{T_H} - \frac{T_{AH}}{T_{ref}}\right)}{1 + \exp\left(\frac{T_{AL}}{T} - \frac{T_{AL}}{T_L}\right) + \exp\left(\frac{T_{AH}}{T_H} - \frac{T_{AH}}{T}\right)}$	
Scaled functional response	$f = \frac{X}{X + X_K}$	
Inter-individual variability	$\{\dot{p}_{Am}\} = \{\dot{p}_{Am}\} \cdot e^{random\ normal(0,sd)}$, $\delta = \delta \cdot e^{random\ normal(0,sd)}$ and $\kappa = \kappa.e^{random\ normal(0,sd)}$ with random normal(0,sd) a normally distributed (mean 0 and standard deviation sd) random number	

Individual-Based Model rules and equations			
Migration rules	*A. marina*	if $E_H < E_H^j$	lugworm in subtidal area $x_i = x_{subtidal}$
		if $E_H = E_H^j$	lugworm recruits on the higher 20% of higher mediolittoral shore $d_x \leqslant d_{max,x}$
		if $E_H > E_H^j$	$bath = -0.29 \cdot TL_{w,i} + 6.60$, if ($x_i > bath_i$ and $d_x \leqslant d_{max,x}$),set $x_i = bath_i$
Migration rules	*A. defodiens*	if $E_H < E_H^p$	black lug in subtidal area $x_i = x_{subtidal}$
		if $E_H = E_H^p$	if $d_x \leqslant d_{max,x}$, black lug moves to random x_i within infralittoral
		if $E_H > E_H^p$	$x_{i,t+1} = x_{i,t}$
Offspring number	$N_{\text{Offspring,emitted},i} = ratio_f.\frac{E_R,i}{E_0}$, if $Capacity_{\text{shore}} \geqslant \sum_{i=1}^{abundance} N_{\text{Offspring,emitted},i}.\dot{s}^{a_j}$		
	$N_{\text{Offspring,shore},i} = N_{\text{Offspring,emitted},i}.\dot{s}^{a_j}$, else $N_{\text{Offspring,shore},i} = \frac{Capacity_{\text{shore}} - Abundance}{N_{\text{spawning}}}$		
	$a_j = 120$ for *A. marina* and $a_j = 110$ for *A. defodiens*, guessed from simulations at Wx		

Individual-Based Model outputs analyses		
Abundance	*Abundance* (N indiv.)	$Abundance_{marina}$ = count(*A. marina*), $Abundance_{defodiens}$ = count(*A. defodiens*)
Total stock biomass	TSB (g)	$TSB = \sum_{i=1}^{n} Ww_i$, with n the abundance in *A. marina* or *A. defodiens*
mean Length at puberty	$L_{p,population}$ (cm)	$L_{p,population} = mean(L_{p,individual})$
Maximum length	$L_{max,population}$ (cm)	$L_{max,population} = mean(L_{max,10\%\ \text{largest individuals}})$
Total reproductive output	TRO (N eggs)	$RO_i = \sum_{t=1}^{\text{end simulation}} N_{\text{Offspring,emitted},i,t}$, $TRO = \sum_{i=1}^{N\text{simulated individuals}} RO_i$
Gravity center of Y	G_Y (m of shore level)	$G_Y = \frac{\sum_{x=x_{min}}^{x_{max}} Y_x.x}{Y}$, Y being the abundance or biomass, x the shore level

Metabolic responses to food and temperature of A. marina. In order to account for the impact of environmental changes on the individuals' metabolism, corrections were made to the rates considered by the model in the equation of fluxes in terms of temperature and food quantity through the Arrhenius temperature and the scaled functional response corrections (Kooijman, 2010, Table 1). The metabolic response to food and temperature of *A. marina* has already been explored (De Cubber et al., 2020). The previous study identified the Arrhenius temperature of *A. marina* within and outside the species temperature tolerance range, and the chlorophyll-a concentration as a good proxy for food, with an associated half-saturation coefficient X_K of 5 µg.L^{-1} (De Cubber et al., 2020).

Metabolic responses to food and temperature of A. defodiens. The effect of temperature on metabolic rates of *A. defodiens* was extrapolated from an oxygen consumption experiment performed on 300 individuals of *A. defodiens* sampled at Wimereux (50°45'N, 1°36'E) from May to July 2019. To do so, a microelectrode Unisense® OX500 coupled to a picoammeter (Unisense PA 2000, Denmark) following De Cubber et al. (2019) with 325 ml containers filled with twice-filtered seawater (TFSW) and with 500 ml containers half-filled with burnt sediment and the rest with TFSW. Five temperatures were tested (10, 13, 16, 20 and 24°C) in these two treatments on 30 individuals per treatment, where lugworms were acclimated 24h prior each respiration measurement. As no *in situ* growth could be followed for this species in order to reconstruct the scaled functional response of the species and identify a relevant proxy for food (De Cubber et al., 2020), the same proxy for food and half-saturation coefficient X_K as for *A. marina* were used as a first approximation.

Inter-individual variability. Inter-individual variability was introduced following Martin et al. (2013) and Koch and De Schamphelaere (2020). A subset of 3 DEB parameters ($\{\dot{p}_{Am}\}$, κ and δ) were considered to follow a normal distribution of the mean estimated value of parameter and standard deviation of 15%, taken from Koch and De Schamphelaere (2020) and leading to relevant size distributions within the population of Wimereux(Eastern English Channel, France). From the original subset of parameters used by Martin et al. (2012), the maturity energy thresholds were removed following Koch and De Schamphelaere (2020) while the shape coefficient was added as it is variable between individuals (see De Cubber et al., 2019; 2020) (Table 1).

2.1.2. DEB parameters estimation for A. defodiens

A. defodiens' DEB parameters were estimated using the covariation method described by Lika et al. (2011), and the data set shown in Sup. Mat. 2. The estimation was completed using the package DEBtool (following Marques et al., 2018) on the software Matlab R2020a using an abj-DEB model. The parameter estimation procedures were evaluated by computing the Mean Relative Errors (MRE), varying from 0, when predictions match data exactly, to infinity when they do not, and the Symmetric Mean Square Errors (SMSE), varying from 0, when predictions match data exactly, to 1 when they do not (http://www.debtheory.org) (Marques et al., 2018).

2.2. Individual-Based Model (IBM)

2.2.1. Description

The ODD framework (Grimm et al., 2020) was followed here for IBM description.

Purpose. The purpose of our IBM was to simulate realistic population dynamics of two species, *A. marina* and *A. defodiens* at one study site with known environmental conditions (here chl-a water concentration and Sea-Surface Temperature) and to infer the latitudinal heterogeneity of the two species' performances from changes in environmental forcings alone.

Process overview. The IBM accounted for different processes influencing the *Arenicola* spp. population dynamics not included in the DEB models such as migration, density restrictions and adult/juvenile mortality (due to ageing, predation, disease or harvesting). Spawning and recruitment were set to happen according to the individual maturity level (obtained from the DEB model), the availability of the stage-related habitat and, in the case of spawning, favourable temperature conditions (Fig. 1). Stochasticity was introduced in the model via inter-individual variability in DEB parameters described previously.

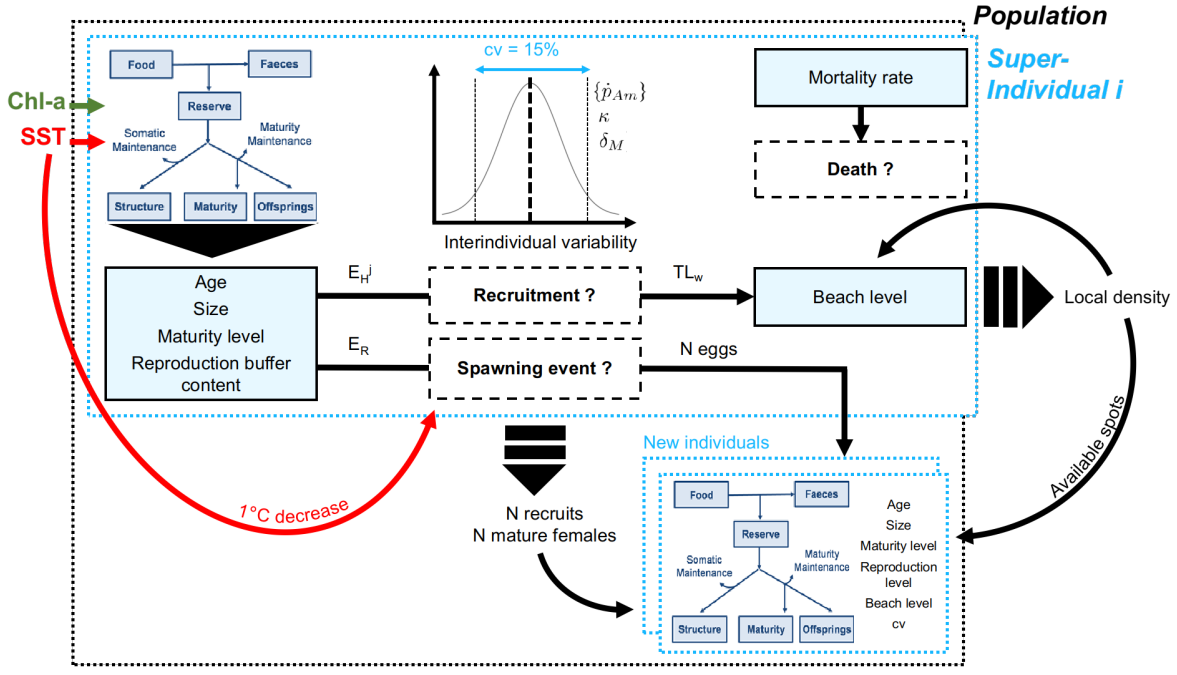

Figure 1: Representation of the different physiological, behavioural and population processes considered in the Dynamic Energy Budget Individual-Based model (DEB-IBM). Chl-a is the chlorophyll-a concentration of the seawater and SST the Sea-Surface Temperature. *cv* is the coefficient of variation around the normal distribution of the DEB parameters $\{\dot{p}_{Am}\}$, the maximum assimilation rate, κ, the allocation fraction to soma, and δ_M, the shape coefficient. E_H^j is the energy threshold of the maturation compartment at which metamorphosis happens. E_R is the energy content in the reproduction buffer. TL_w is the trunk length of super-individuals and N stands for number.

Entities. In order to reduce calculation times, *A. marina* and *A. defodiens* super-individuals were created. Since shore location on the beach for *A. marina* depends on its length and local density (see below) we could not define a single super-individual per cohort and instead simulated a greater

number of super-individuals accounting for a fixed number of individuals. Each super-individual possessed a set of parameters, and all the individuals represented by a super-individual shared the same state variable values. The number of individuals represented by a super-individual allowed for low densities to occur at fine scale and was defined at the study site Wimereux (Eastern English Channel, France), where each super-individual would not account for more than 1% of the population. Given the potential discrepancies in density between the two species and the maximum densities per shore level observed (De Cubber et al., 2018; Pires et al., 2015), one super *A. marina* individual accounted for 16 individuals and one super *A. defodiens* individual accounted for 4 individuals. Each super-individual possessed a set of DEB parameters and its related State Variables (Table 1) were computed at each time step along with its location on the foreshore, its survival and the production of new individuals (Fig. 1). The overall population dynamics was considered as the sum of each individual dynamic (Fig. 1).

Space. Population dynamics were simulated on the same hypothetical shore based on the one existing at Wimereux (Eastern English Channel, France), where numerous ecological studies (e.g. structure of population, density, reproduction, migration...) have been carried out. Its dimensions were of 1 meter large and 600 meters long (Fig. 2, see De Cubber et al., 2018, 2019 and 2020 for further details). On this shore, subtidal level is under 0m of bathymetry, infralittoral level is above the subtidal level up to 200m from the subtidal level limit and +2m of bathymetry, mediolittoral inferior level is above the infralittoral level up to 200m from the infralittoral level limit and +4m of bathymetry, and mediolittoral superior level is above the mediolittoral inferior level up to 200m from the mediolittoral inferior level limit and +6m of bathymetry (constant slope, Fig. 2).

Individual-based processes for A. marina*.* *A. marina*'s adults spawned on the shore (see 1 in Fig 2 b). In order to define spawning dates for *A. marina*, we used spawning dates reported by various authors at two locations (France and Scotland), and considered that spawning was a result of a certain value of decreasing temperature and a certain gonado-somatic index (in this case, GSI was the wet weight of gametes divided by the total wet weight of the individual) as these two parameters are usually used in reproduction buffer emptying rules (Pethybridge et al., 2013; Watson, 2000). The maximum number of new individuals was set according to DEB results and until recruitment, larvae remained in the subtidal environment. Larval mortality was supposed to be 0.06 indiv.d^{-1} (Ellien, 2004). Recruitment was set to happen at metamorphosis ($E_H = E_H^j$) (see 2 in Fig 2 b). Recruits of *A. marina* settled on the high mediolittoral shore following several authors' observations (Fig. 2, Sup. Mat. 1, De Cubber et al., 2018; 2020; Farke and Berghuis, 1979 a; b; Newell, 1949; 1948; Reise, 1985; Reise et al., 2001)). Down-shore migrations of juveniles and adults of *A. marina* were simulated based on the previous study of De Cubber et al. (2020) using the relationships between the length of the worms and the bathymetry of the shore level (see 3 in Fig. 2). For juvenile and adult stages, survival and mortality rates were also poorly known and might vary.

Therefore, we considered a constant mortality rate for both adults and juveniles for *A. marina* derived from field observations (parameter estimation is described hereafter).

Individual-based processes for A. defodiens. As almost no data was available regarding environmental or biological triggers for *A. defodiens*' spawning events, spawning was forced each year in mid-December for this species (see 1 in Fig. 2 c).

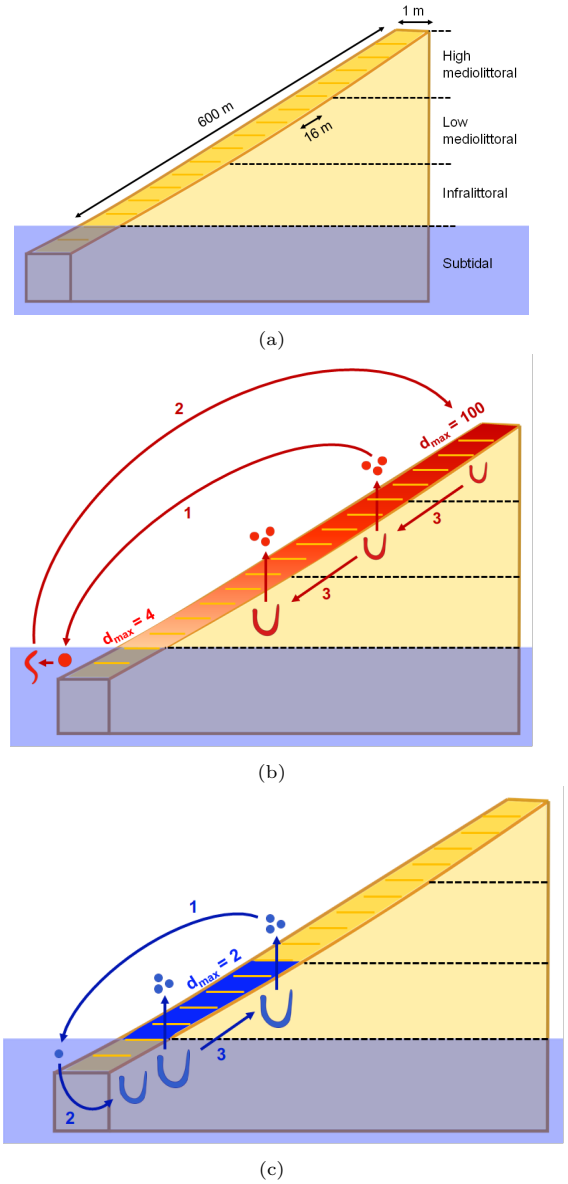

Figure 2: Simulated shore features in terms of grid definition, shore levels and shore length (a), associated uses of the shore by the different life stages and maximum density settings (d_{max} in $individuals.m^{-2}$) of (b) *A. marina* and (c) *A. defodiens*. For *A. marina*, numbers relate to (1) spawning, (2) recruitment and (3) shore migration. For *A. defodiens*, they relate to (1) spawning, (2) subtidal settlement and (3) shore colonisation at adult stage. Cells dimensions were 1 m large and 4 m long. For representation concerns, the number of cells represented is not realistic. U-shaped individuals are adults, S-shaped individual are larvae and O-shaped individuals are embryos. Cell density d is calculated as the number of individuals within each grid cell at each time step. For *A. marina*, d_{max} varies linearly along the foreshore between 100 $individuals.m^{-2}$ on the upper foreshore and 4 $individuals.m^{-2}$ on the lower foreshore. For *A. defodiens*, d_{max} (2 $individuals.m^{-2}$) is constant over the infralittoral foreshore (the species cannot colonise the mediolittoral foreshore).

The maximum number of new individuals was set according to DEB results and larvae remained in the subtidal environment (see 2 in Fig. 2 c). Larval mortality was supposed to be 0.06 indiv.d^{-1} (Ellien, 2004). Recruitment was set to happen at metamorphosis ($E_H = E_H^j$). Recruits of *A. defodiens* remained in the subtidal habitat until sexual maturation ("puberty"). Adults of *A. defodiens* reached randomly the infralittoral shore once puberty was reached ($E_H = E_H^p$), and remained there until their death (see 3 in Fig. 2 c, Sup. Mat. 1) (Table 1). Since *A. defodiens* live in deeper galleries and because no data was available regarding mortality rate for the species, we used the same value than for *A. marina* but divided by 2.

Density-dependant processes and interactions. Density-dependent processes such as recruitment have been reported for *A. marina* and might be linked to competition for food, or stability of the gallery within the sediment (Reise et al., 2001; Flach and Beukema, 1994). Maximum densities per shore level occupied by the two species were set according to empirical and literature data (De Cubber, 2018; Pires et al., 2015) (Fig. 1). Local densities at each time step and each cell of the shore grid were calculated and compared with the maximum possible density within each cell to determine if new arrivals through recruitment or migration could happen in the targeted cell,(Table 1). The number of new offspring produced and simulated by one female was also set according to the number of available spots on recruitment grounds (all species considered) rather than according to the real number of offspring produced by each female according to the DEB model. In detail, if the number of offspring potentially emitted (simulated by the DEB model) surviving until metamorphosis was superior to the number of available spots on recruitment grounds, the number of offspring simulated was set equal to the number of available spots on recruitment grounds at this time step times 2 (to avoid cases where early mortality would lead to a number of recruits inferior to the number of available spots on recruitment grounds), divided by the number of females spawning at the same time step (Fig. 1, Table 1). Otherwise, it was set equal to number of offspring emitted simulated by the DEB model. Inter-specific competition could happen when large *A. marina* individuals would reach available spots on the infralittoral shore, hence limiting the number of spots available for *A. defodiens* individuals.

Computation and initialisation. The DEB-IBM was run ten times at each of the 28 study sites in order to account for stochastic variations in the model outputs on NetLogo 6.2.0 software (https://ccl.northwestern.edu/netlogo/). The model was initialised with a first pool of 600 *A. marina* super-individuals (larvae) and a first pool of 90 *A. defodiens* super-individuals (larvae) allowing populations to colonise the shore and survive until the next year. Simulations were run over 20 years with a daily time step (the first 10 years were run for model stabilisation and the outputs of the last 10 years were used for results analyses). Subsequent data analyses and statistical analyses were performed on Matlab R2020a.

2.2.2. Parameter estimation

Three parameters were estimated: the GSI, the fall of temperature, both controlling the spawning events, and the daily mortality rate, regulating death for *A. marina only*. First, the daily mortality rate, $\dot{m}$, was adjusted with a constant spawning period in mid-September as observed at Wimereux (Wx, France, Eastern English Channel), where values from 1 10^{-4} indiv.d^{-1} to 2.5 10^{-3} indiv.d^{-1} were tested (Sup. Mat. 3.1), close to what was observed in the literature (Then et al., 2015). The daily mortality rate was assessed on the basis of a relationship between simulated mean density and mortality rate for the Wx reference site (6.5 indiv.m^{-2}, De Cubber et al., 2018). The daily mortality value obtained from this model was used for all sites in this study (Sup. Mat. 1).

Second, the GSI and the fall of temperature were assessed by testing a decrease rate from 0 to 2°C in 2 weeks' time (0.25°C increment) and a GSI from 0.05 to 0.16 (0.01 increment) all together (Sup. Mat. 3.2). Each couple of values were considered consistent with observations when 80% of the spawning events happened between early September and early December at Wx and at East Sands (St Andrews, Scotland) (De Cubber et al., 2018; Watson et al., 2000). In case further choice was needed, the parameters leading to a GSI of 0.1 were used, close to previous values reported at Wx (De Cubber et al., 2019).

2.3. Environmental data

Daily Sea-Surface Temperature (SST, 4 km² resolution : www.cersat.ifremer.fr) and monthly chlorophyll-a concentration (chl-a, 1 km² resolution : www.hermes.acri.fr) time series were extracted from satellite data at 28 locations where lugworms have been described (Fig. 3 and Sup. Mat. 4) over a 10 years' time period (2010-2020).

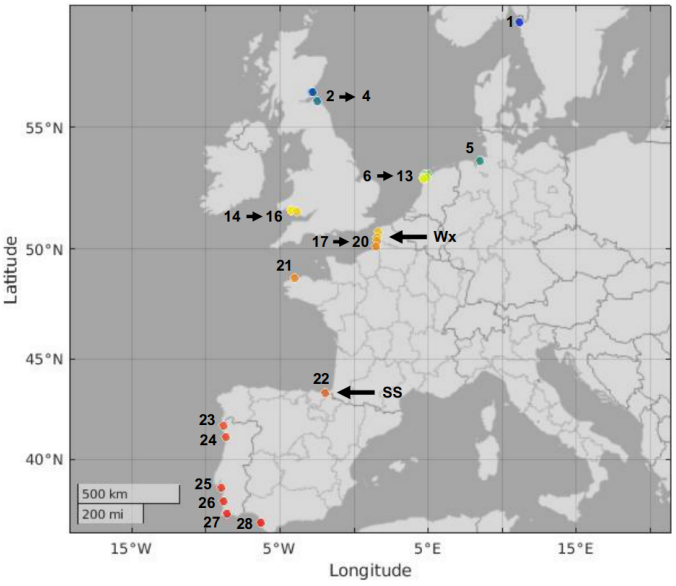

Figure 3: Studied sites (and site number) from the North East Atlantic where lugworm populations dynamics and biological traits were investigated according to local Sea-Surface Temperature and Chlorophyll-a data. Sites correspond to areas where *A. marina* and/or *A. defodiens* were described.Further details on the sites are given in Sup. Mat. 4. Sites colours are used hereafter in the results section. On black sites, environmental data were not available or their resolution was too low, and no simulations were run.

Only sites where the extracted data covered more than 30% of the time series were kept in the study. In order to allow simulations to stabilise over the simulation period (which took around 9 to 10 years), they were performed using two cycles of 10 years. For each site, only one cell of each environmental forcing map was used. When one SST data point was missing and in between monthly chl-a values, interpolations were made on Matlab R2019a using the Interp1 function (simple linear method used for Temperature as missing values were scarce, and Modified Akima cubic Hermite interpolation used for chl-a concentration values, allowing for some undulations).

2.4. DEB-IBM output analyses

2.4.1. Model stability

The number of simulation runs needed was assessed according to Ritter et al. (2011). 52 runs of the model were made at one studied site (Wimereux). 1000 groups of 2 to 50 runs among the 52 runs performed were selected with a bootstrap method. Mean of mean abundance in between group sizes as well as variations in mean abundance in between groups were computed through the standard deviation of means (σ) and the standard error of means (SEM, Equation 1). SEM differences between group sizes N and $N-1$ were also computed. The number of runs chosen allowed SEM stability (Sup. Mat. 5).

$$SEM = \sigma/\sqrt{N} \tag{1}$$

2.4.2. Latitudinal patterns of biological traits

At each site for both species, the mean abundance and biomass, the variations in abundance and biomass, the total reproductive output (TRO), the maximum length ($L_{max,population}$), the length at puberty ($L_{p,population}$), and the spawning periods were extracted from model outputs. The mean abundance and biomass were the means per site over the last 9 years of the simulation. The variations of mean abundance and biomass (total stock biomass, TSB) were the daily values of abundance and biomass over the last 9 years of the simulation. TRO was computed as the sum of the number of oocytes spawned per all simulated lugworm during the period of simulation at each location. $L_{max,population}$ at death per site and per period was computed as the mean of the higher 10% values of the length at death of lugworms. $L_{p,population}$ was computed as the mean length at puberty of all the individuals that had been simulated at one location for one species (Table 1). For the spawning periods, at each location, a Gaussian curve was fitted over the daily number of lugworms spawning per Julian day (1 to 365) over the last 10 years of the simulation with the Matlab R2020a function *fitdist*, after checking that each data set could be represented by a standard and normal distribution with a one-sample Kolmogorov-Smirnov test (Matlab R2020a function *kstest*).

2.4.3. Fine-scale biological traits per location

For two sites with contrasted model predictions (site 17: Wimereux and 22: San Sebastian, see Fig. 3 and Sup. Mat. 4 and 6), the mean shore levels occupied (gravity centre) in terms of

biomass and abundance for each species were calculated at each time step (every day) (see Table 1), Y being the biomass or the abundance of the species at the considered site, x the bathymetry, Y_x the biomass or abundance at bathymetry x, and G_Y the center of gravity of Y (mean bathymetry). The size (0.5 cm trunk length classes) distribution on the shore for each species at each time step was also recorded at these sites.

2.4.4. Influence of chlorophyll-a concentration and temperature

The same model outputs were computed using the environmental variables' time series showing the highest, lowest and median mean values over the whole time period. Biological trait values corresponding to those 9 conditions (3 chl-a conditions x 3 SST conditions) were compared calculating the index $i = \frac{trait\ value - min(trait\ value)}{max(trait\ value) - min(trait\ value)}$ varying from 0 to 1.

3. Results

3.1. Environmental variables

The mean values of SST and concentration of chl-a per site over the period 2010-2020 highlighted some contrasted latitudinal gradients, where the highest SST values were found beneath latitude 45° N whilst the highest chl-a values were found above latitude 50° N (Fig. 4 a and b, Sup. Mat. 7.1 and 7.2). There were some exceptions in the chl-a gradient, with values sometimes higher close to some south estuaries (North Coast of Portugal) (Fig. 4 b, Sup. Mat. 7.1). Each site displayed the same seasonal SST pattern with highest SST values in summer and lowest SST values in winter (Fig. 4 c). Chl-a also displayed some seasonal pattern with pikes between March and September but some variations in-between sites could be observed (Fig. 4 d).

3.2. Model parameters

3.2.1. Calibration of DEB parameters of A. defodiens

The parameter estimation of the abj-DEB model for *A. defodiens* provided a MRE of 0.19 and SMSE of 0.27 (Sup. Mat. 2). All data used for model calibration are freely available within the Add-my-Pet collection (https://bio.vu.nl/thb/deb/deblab/add_my_pet /index.html) and in Sup. Mat. 2. DEB parameters of *A. defodiens* (and *A. marina*) are provided in Table 2.

3.2.2. Calibration of DEB-IBM parameters

Mortality $\dot{m}$ of juveniles and adults of *A. marina* at Wimereux was estimated at 8.16 10^{-4} indiv.d^{-1} (Table 2, Sup. Mat 3.1). The values of decrease of SST over two weeks (T_{spawn}) and GSI threshold ($GSI_{trigger}$) simulating more than 80% of the lugworms spawning within the main observed spawning period (end of August to beginning of December) were respectively of 1°C per 14 days and 0.1 (Table 2, Sup. Mat. 3.2).

3.3. Latitudinal population responses to environmental parameters

3.3.1. Population abundance and biomass

After simulation over the 28 studied sites, *A. marina*'s population density (abundance.m^{-2}) and TSB appeared the highest above the latitude 49° N and in Northern Portugal, and the lowest in Southern Spain and Portugal as well as in France below latitude 49° N (Figs. 5 a, b), but not leading to any populations' crashes (Figs. 6 a, c).

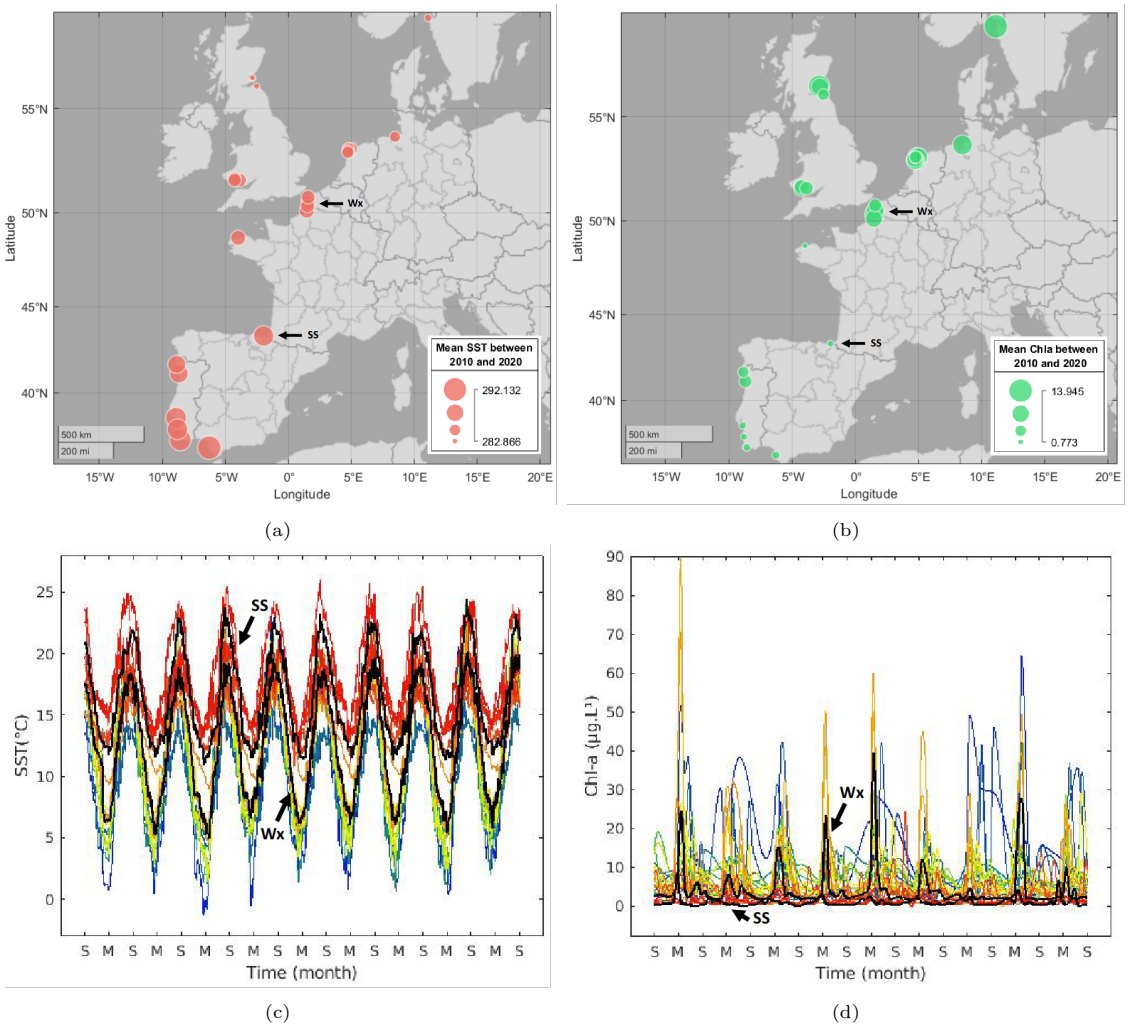

Figure 4: (a) Mean Sea-Surface Temperature (SST, K) and (b) Chlorophyll-a concentration ($chl-a$, µg.L^{-1}) between 2010 and 2020 at each of the 28 sites where lugworms occurrences were recorded. (c) Associated SST variations and (d) Chl-a variations at each site between 2010 and 2020 (S stands for September and M for March), from higher latitudes in blue to lower latitudes in red. Variations in both environmental variables are represented in black at Wimereux (Wx) and San Sebastian (SS). Both environmental forcings were obtained from satellite data (respectively extracted from www.cersat.ifremer.fr at a 4 km² resolution and from www.hermes.acri.fr at a 1 km² resolution).

For *A. defodiens*'s population, density (abundance.m^{-2}) and TSB appeared the highest above the latitude 45° N and in Northern Portugal, and the lowest in Southern Spain, Portugal and in France below latitude 45° N (Figs. 5 c, d), where simulations led to a population crash (Figs. 6 b, d). Population crashes either happened from the beginning of the simulation, in this case initialized individuals did not survive, either at other times of the simulation when overall density

was high some time before (Sup. Mat. 8). Overall, population crashes seemed associated to low levels of chl-a associated to high SST (Sup. Mat. 8).

Table 2: Summary of the primary and some auxiliary parameters of the abj-Dynamic Energy Budget models as well as the Individual-Based model for *A. marina* and *A.defodiens*. TTR stands for Temperature Tolerance Range, MT for Maturation Threshold.

		A. marina	*A. defodiens*	
Parameter	Symbol	Value	Value	Unit
Dynamic Energy Budget parameters				
Reference temperature[1]	T_{ref}	293.15[b]	293.15[a]	K
Fraction of food energy fixed in reserv10[1]	κ_X	0.80[b]	0.80[a]	-
half-saturation coefficient for chl-a	X_K	5.00[b]	5.00[b]	µg.L^{-1}
Arrhenius temperature	T_A	4014[b]	4568[a]	K
Arrhenius temperature under the TTR	T_{AL}	69080[b]	-	K
Arrhenius temperature over the TTR	T_{AH}	82380[b]	-	K
TTR's lower boundary	T_L	272.8[b]	-	K
TTR's higher boundary	T_H	297.7[b]	-	K
Energy conductanc10[2]	$\dot{v}$	9.77 10^{-03}[b]	0.0207[a]	$cm.d^{-1}$
Allocation fraction to soma	κ	0.90[b]	0.83[a]	-
Reproduction fraction fixed in eggs[1]	κ_R	0.95[b]	0.95[a]	-
Volume specific costs of structure	$[E_G]$	4123[b]	4209[a]	$J.cm^{-3}$
MT for the trochophore larva	E_H^{tr}	1.11 10^{-03}[b]	8.69 10^{-04}[a]	J
MT for birth	E_H^b	1.77 10^{-03}[b]	1.03 10^{-03}[a]	J
MT for metamorphosis	E_H^j	3.19[b]	3.52[a]	J
MT for puberty	E_H^p	104.10[b]	12.32[a]	J
Acceleration rate[3]	s_M	12.13[b]	14.92[a]	-
Maximum assimilation rate [2]	$\{\dot{p}_{Am}\}$	10.99[b]	8.89[a]	$J.cm^{-2}.d^{-1}$
Specific somatic maintenance rate	$[\dot{p}_M]$	15.6[b]	28.87[a]	$J.cm^{-3}.d^{-1}$
Maturity maintenance rate [1]	$\dot{k}_J$	2.00 10^{-03}[b]	2.00 10^{-03}[a]	d^{-1}
Shape parameter until birth	δ_{Me}	0.66[b]	0.66[b]	-
Shape parameter after metamorphosis	δ_M	0.231[b]	0.1601[a]	d^{-1}
Specific density of wet structure [1]	d_V	1[b]	1[a]	$g.cm^{-3}$
Specific density of wet reserve [1]	d_E	1[b]	1[a]	$g.cm^{-3}$
Specific density of dry reserve [1]	d_{Ed}	0.16[b]	0.16[a]	$g.cm^{-3}$
Specific chemical potential of dry reserve [1]	μ_{Ed}	550000[b]	550000[a]	$J.Cmol^{-1}$
Molar weight of dry reserve [1]	w_{Ed}	23.9[b]	23.9[a]	$g.Cmol^{-1}$
Inter-individual variability coefficient	c_v	15[a]	15[a]	%
Individual-Based Model parameters				
Gonado-Somatic Index spawning threshold	$GSI_{trigger}$	10[a]	-	%
Temperature decrease spawning threshold	ΔSST_{14}	1[a]	-	$K.14d^{-1}$
Mortality rate	$\dot{m}$	8 . 10^{-04}[a]	4 . 10^{-04}[a]	$indiv.d^{-1}$
Maximum local density - high mediolittoral	d_{max}^{high}	100[c]	-	$indiv.m^{-2}$
Maximum local density - low infralittoral	d_{max}^{low}	4[c]	-	$indiv.m^{-2}$
Maximum local density - subtidal	d_{max}^{sub}	4[c]	2[c]	$indiv.m^{-2}$
Larval survival rate	$\dot{s}$	0.94[d]	0.94[d]	$indiv.d^{-1}$
Female ratio	$ratio_f$	0.5	0.5	-

[1] Fixed parameters. The values were taken from the generalized animal (Kooijman, 2010).
[2] These are the values at birth
[3] s_M is given for a scaled functional response of 1 after metamorphosis
References associated to the parameter values: [a]This study, [b]De Cubber et al. (2020), [c]De Cubber et al. (2018) and [d]Ellien et al. (2004)

For *A. marina*, yearly variations in abundance and TSB could be observed at most sites where abundances exceeded 1000 individuals due to recruitment (Fig. 6 a), whilst they were much more reduced for *A. defodiens* (Fig. 6 b). Indeed, for the latter species, individuals could remain on the

subtidal environment and colonise the infralittoral foreshore as soon as densities allowed it (empty spots).

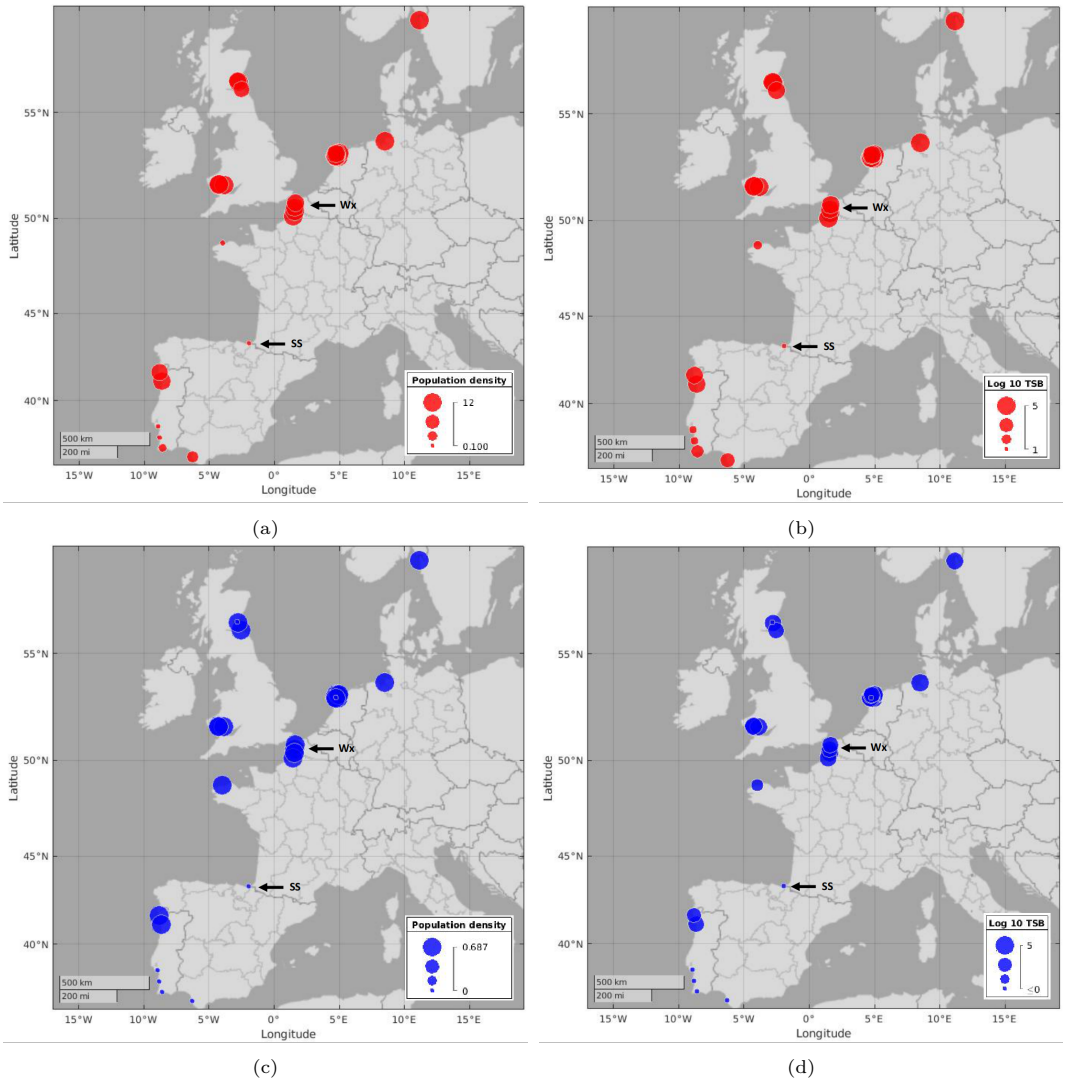

Figure 5: Projections of mean population density (individuals.m^{-2}, left) and log 10 total stock biomass TSB (juveniles + adults) (g, right) of *A. marina* (top, red) and *A. defodiens* (bottom, blue) at the 28 studied locations between 2010 and 2020 of the Dynamic Energy Budget Individual Based Model developed in this study.

3.3.2. Total reproductive output

TRO overall displayed the same latitudinal patterns than abundance and TSB for both species, with up to 4 orders of magnitude of difference between the highest and the lowest values for *A. marina* and 10 (as some populations crashed and could not produce offspring, see sites 26 and 29) for *A. defodiens* (Fig. 7).

3.3.3. Maximum length and length at puberty

The mean $L_{p,population}$ varied between 2.5 (San Sebastian, Spain) and 3 cm (northern sites) for *A. marina* and between 0 (Roscoff, France) and 1.6 cm (northern sites) for *A. defodiens* (Figs. 8 a and c).

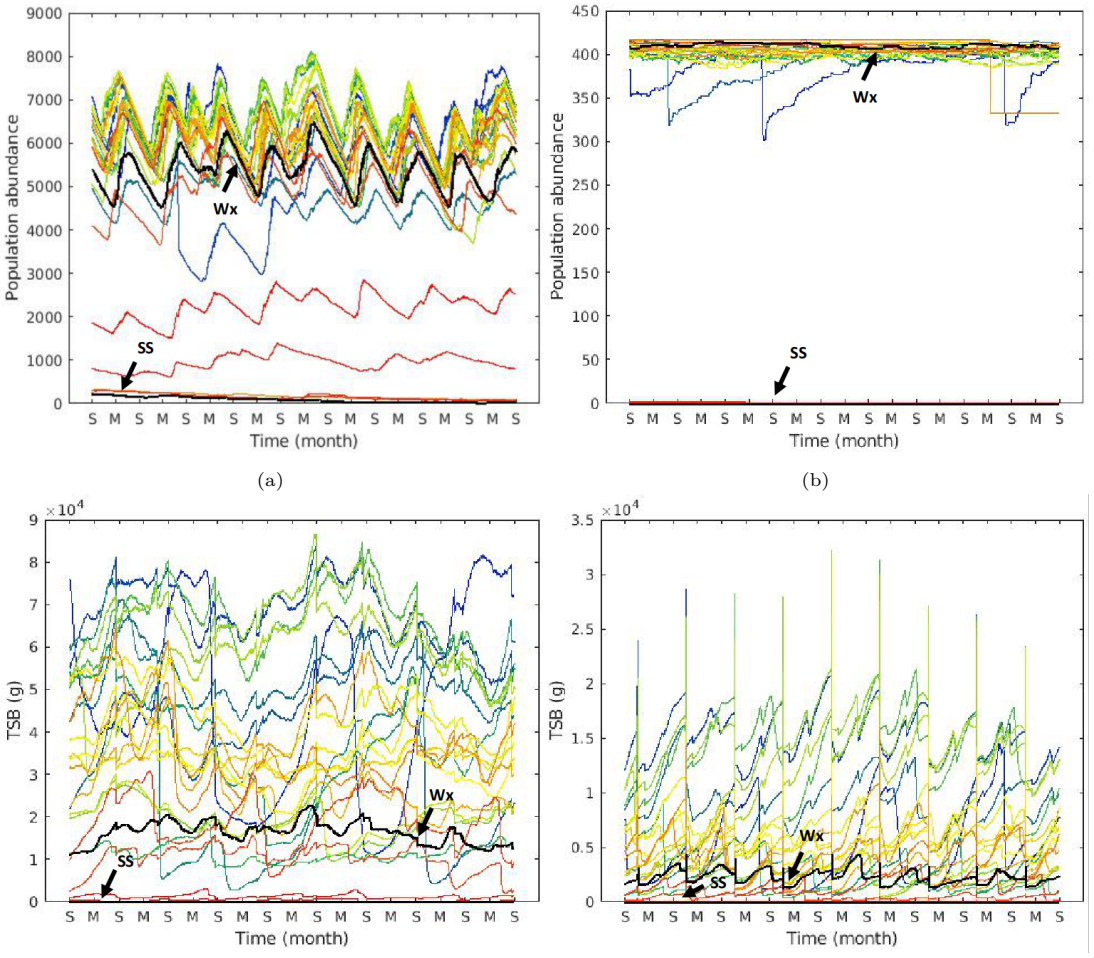

Figure 6: Projection of the evolution of *abundance* (number of individuals on the foreshore) (a, b) and Total Stock Biomass (TSB, g) (c, d) at the 28 studied locations for *A. marina* (left, a, c) and *A. defodiens* (right, b, d) from 2010 to 2020 (S stands for September and M for March). Coldest colors stand for sites of the highest latitudes and warmest colors for the sites of the lowest latitudes (see Fig. 3).

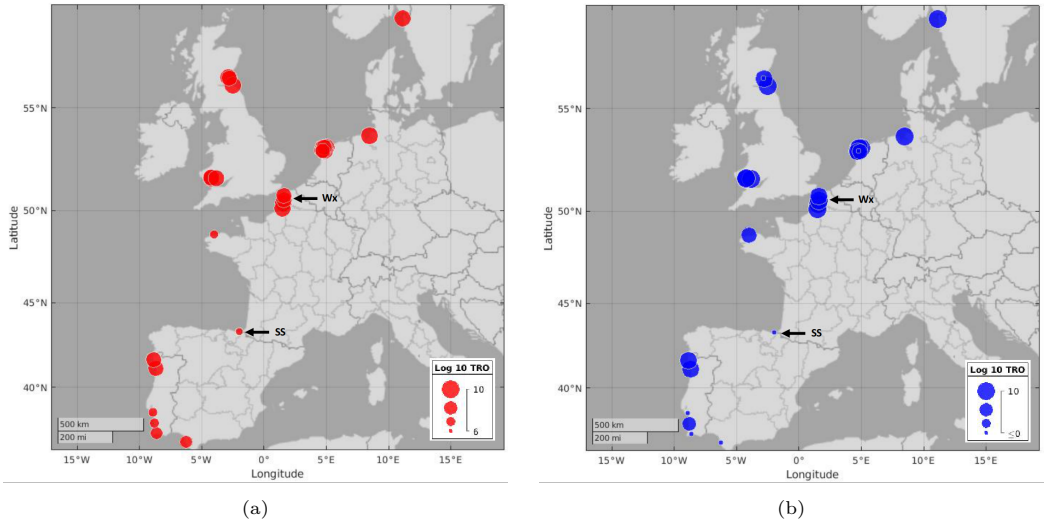

Figure 7: Projections of total reproductive output (TRO) of *A. marina* (left, red) and *A. defodiens* (right, blue) at the 28 studied locations between 2010 and 2020 of the Dynamic Energy Budget Individual Based Model.

$L_{max,population}$ followed a similar pattern, varying between 3.3 and 12 cm for *A. marina*, with minimum and maximum at the same locations, and between 0 (San Sebastian, Spain, where populations crashed) and 13.4 cm for *A. defodiens* (also at northern sites) (Figs. 8 b and d). Both biological traits displayed the same latitudinal patterns described for abundance, TSB and TRO, the minimal values of $L_{p,population}$ being obtained where individuals reached the lowest sizes.

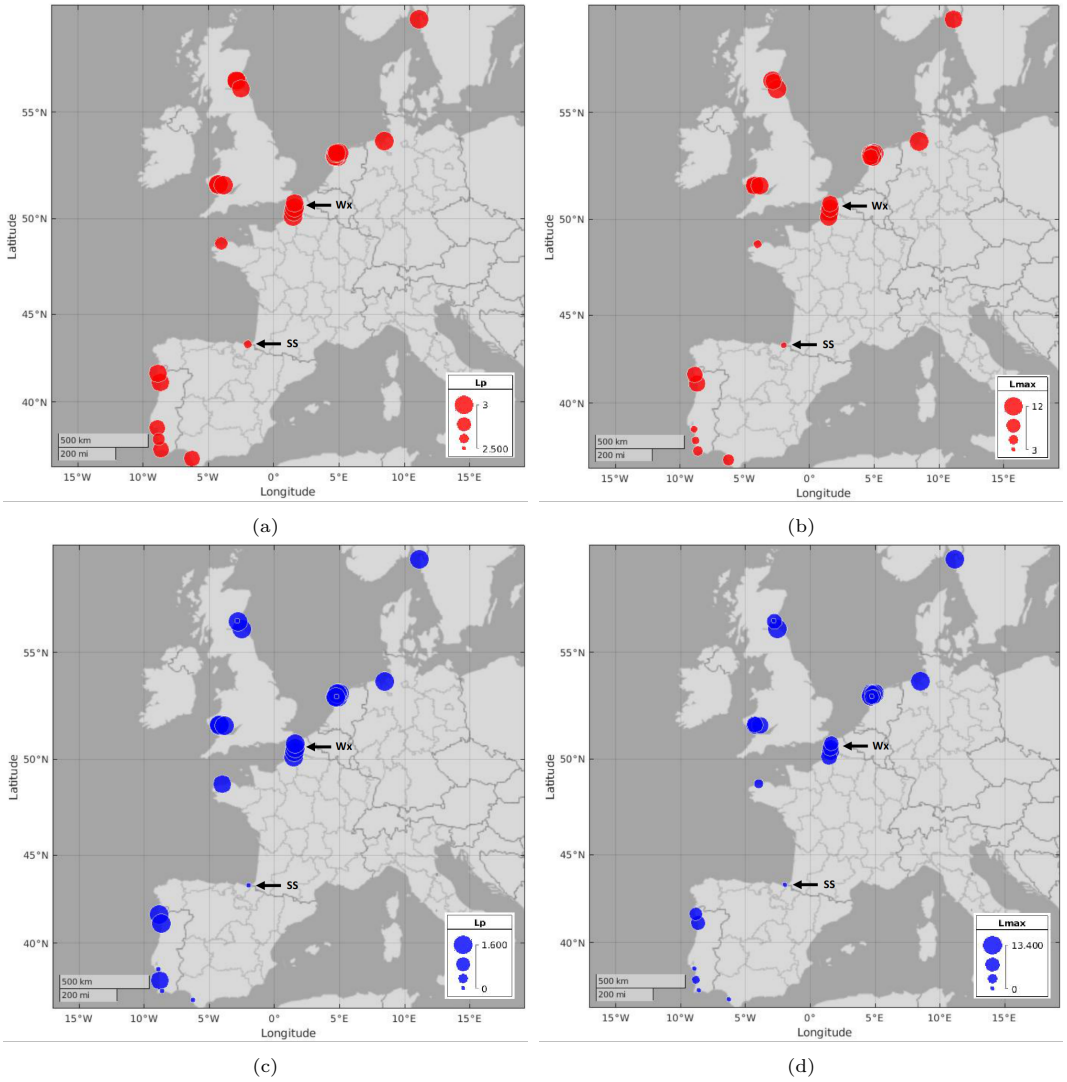

Figure 8: Projections of mean length at puberty $L_{p,population}$ (cm, left) and mean length of the 10% longer individuals $L_{max,population}$ (cm, right) of *A. marina* (top, red) and *A. defodiens* (bottom, blue) at the 28 studied locations between 2010 and 2020 of the Dynamic Energy Budget Individual Based Model developed in this study.

3.4. Influence of chlorophyll-a concentration and Sea-Surface Temperature

Population responses of *A. marina* and *A. defodiens* in terms of the five targeted biological traits (*abundance*, TSB, $L_{p,pop}$, $L_{max,pop}$ and TRO) to different scenarios of mean SST and chl-a were compared. The relative outputs (maximum diameter corresponding to the higher value and minimum diameter to the lower value of the biological trait) followed the same pattern for all biological trait except *abundance*: biological trait values increased with increasing chl-a levels and, to a much lesser extent, with increasing SST (the latter pattern was mainly observable for TRO).

Overall, chl-a had more influence than SST on all biological traits for both species (Fig 9). However, populations' responses to chl-a and SST in terms of abundance were different between species: populations of *A. marina* reached high abundance when chl-a $\geqslant$ 5 µg.L^{-1}, whilst populations of *A. defodiens* did not display clear pattern for abundance with neither chl-a concentration nor SST. As abundance values for *A. defodiens* varied between 334 to 416 individuals (same level of magnitude) when those for *A. marina* varied between 34 to 6408 individuals, low abundance of *A. defodiens* did not impact greatly TSB. The fact that TSB and other biological traits followed the same trends for *A. defodiens* and for *A. marina* seems to point out that the abundance pattern observed for *A. defodiens* is linked to the interplay between environmental parameters and competition for space with large individuals of *A. marina* on the infralittoral foreshore (that manage to grow and reach this shore level only in the best environmental conditions).

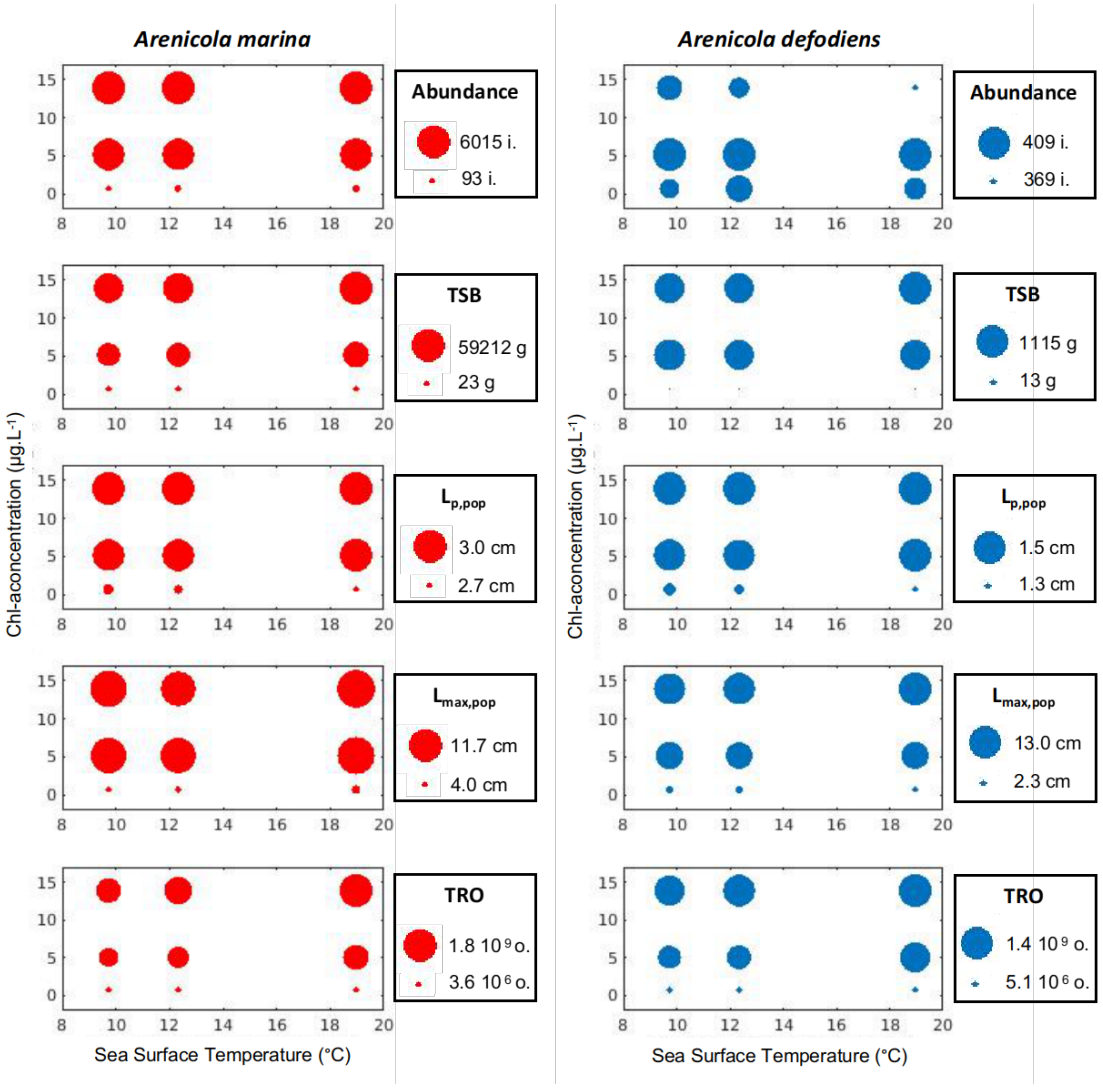

Figure 9: Relative values of mean abundance, mean total stock biomass (TSB), mean length at puberty ($L_{p,pop}$ or $L_{p,population}$), maximum length ($L_{max,pop}$ or $L_{max,population}$), and total reproductive output (TRO) of populations simulated with the 9 scenarios of chlorophyll-a concentration and Sea-Surface Temperature for *A. marina* (red, left), and *A. defodiens* (blue, right).

3.5. Fine-scale underlying mechanisms

Different patterns in populations' biological traits were observed such as at Wimereux (Wx) and San Sebastian (SS) (Fig. 3). The corresponding population dynamics were investigated more closely in terms of life-stage dynamics, shore colonisation and inter-individual variability.

3.5.1. Life-stage dynamics of A. marina

For *A. marina*, the typical pattern of yearly spawning (embryo/trochophore larva pikes) around September and recruitment (juvenile waves) in spring documented at Wx were accurately reproduced by the DEB-IBM, with the adult population remaining quite stable around 4000 individuals yearly renewed every year by the arrival of new individuals (Fig. 10). However, at SS, spawning events did not occur every year and the adult population appeared extremely low and variable with 150 down to 20 individuals. There, only a very small, if not negligible, portion of the population managed to spawn and population decreased (Fig. 10).

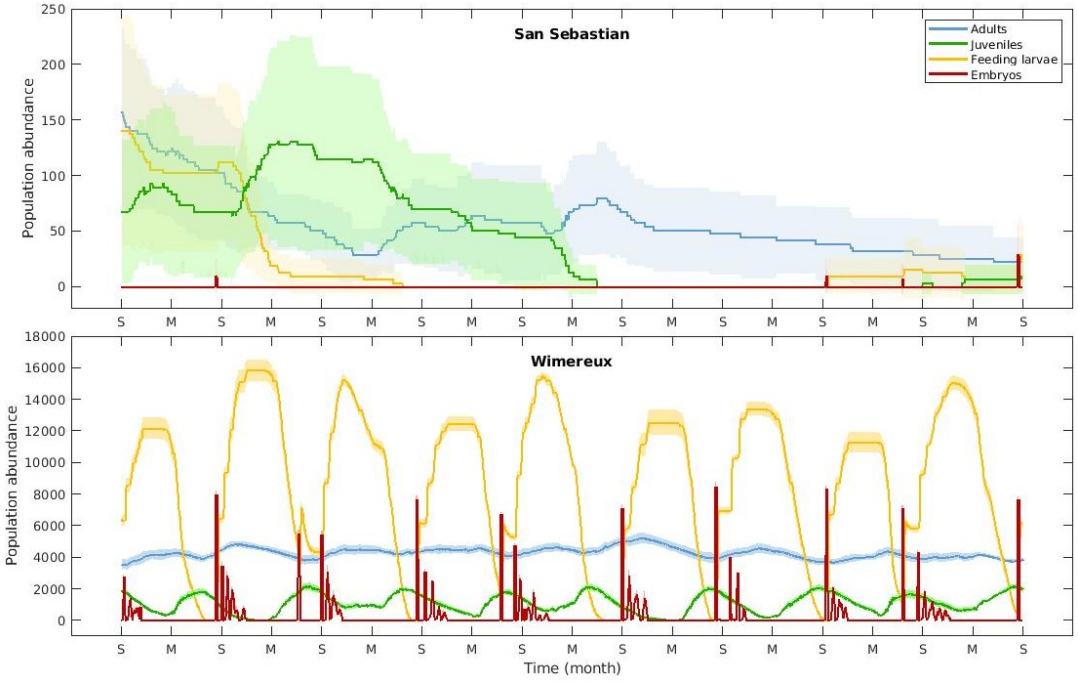

Figure 10: DEB-IBM simulated abundance of embryos (dark red), feeding larvae (yellow), juveniles (green) and adults (blue) according to time (S stands for September and M for March) of two populations of *A. marina*: San Sebastian (Spain, top) and Wimereux (France, bottom). Lines correspond to the mean value obtained from the 10 simulations, shaded areas upper and lower limit correspond to more or less one standard deviation.

3.5.2. Shore colonisation

The simulated mean bathymetry occupied on the foreshore by *A. marina* displayed different patterns between Wimereux (Wx) and San Sebastian (SS) as well (Fig 11). At Wx, the number of lugworms was simulated higher on the mediolittoral superior foreshore once a year (corresponding to the typical pattern for recruitment) and then individuals migrated down to the lower infralittoral shore, the mean bathymetry occupied at this point being also influenced by the presence of larvae in the subtidal environment (Fig. 11). At SS, the fine scale distribution pattern was quite different

with no clear recruitment pattern as previously described in Fig. 10. There, a high proportion of lugworms in the simulated population occupied the higher shore for the first four years as juveniles were more numerous than adults at this point (see Fig. 10). When adults started to be in the majority, their lower shore level remained higher than at Wimereux linked to a lower mean maximum size, as shore migration is linked to length for this species (see Fig. 8b).

At Wx, the mean shore levels of *A. defodiens* remained difficult to analyse because of the non-negligible subtidal pool of individuals for this species (Fig. 11). However, it appeared that both species occurred on the infralittoral shore at least part of the year (Fig. 11). Inter-specific interactions were therefore further studied.

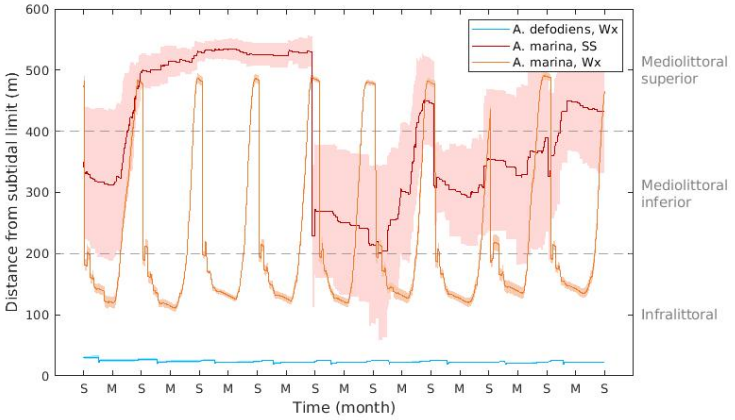

Figure 11: Mean shore level (expressed in m from subtidal limit) simulated in terms of abundance for *A. marina* and *A. defodiens* obtained at Wimereux (orange, blue) and San Sebastian (dark orange).

3.5.3. Density-dependant recruitment of A. marina

For *A. marina*, the number of juveniles (recruits of the year) was related to the number adults on the foreshore (Fig. 12).

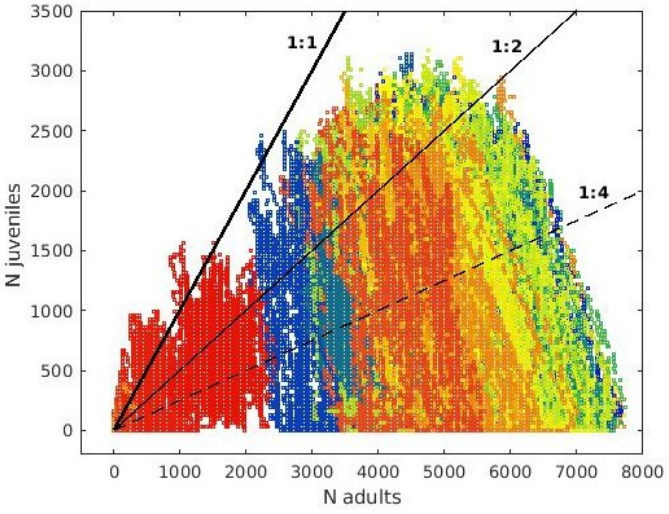

Figure 12: Number of juveniles according to the number of adults on the shore (b) at the 28 sites (coldest colors stand for sites of the highest latitudes and warmest colors for the sites of the lowest latitudes) at each time step.

At southern sites with overall low number of adults (⩽1000 individuals), the proportion of juveniles reached values superior to 50% as adult lugworms did not survive a really long time there (Fig. 12). Overall, the maximum number of juveniles increased with the number of adults until adult populations levels around 5000 individuals. At this point, their numbers could reach more than 3000 individuals (Fig. 12). Indeed, the more abundant is the species, the higher is its maximum length, hence the lower its level on the shore is, leaving more space for juveniles to recruit. For populations above 5000 adults, the maximum number of juveniles and their proportion decreased revealing density-limiting recruitment for these populations (Fig. 12).

3.5.4. Inter-specific interactions

Inter-specific interactions were explored focusing on the relations between mean simulated abundances of *A. defodiens* and mean simulated abundances and minimum shore level occupied by *A. marina* (Fig. 13).

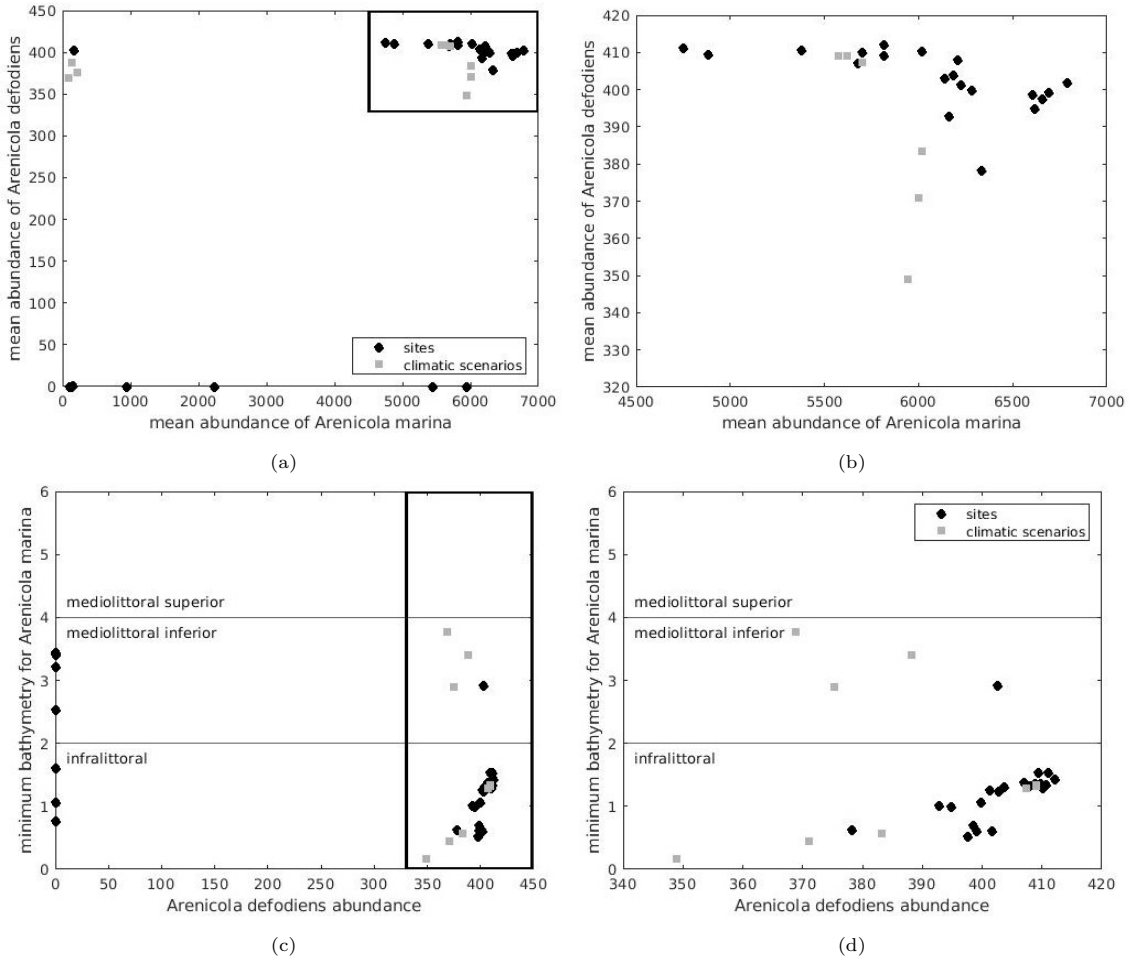

Figure 13: Mean abundance of *A. defodiens* according to the mean abundance of *A. marina* (a, b) and minimum bathymetry (m) of *A. marina* according to the abundance of *A. defodiens* (c, d) simulated at the 28 studied sites (black dots) and for the 9 climatic scenarios (grey squares). Boxes in Figs a and c represent the axes of Figs b and d. Horizontal lines in Figs c and d are the limit of the foreshore levels.

It appeared that, when environmental conditions allowed it (boxes on Figs. 13 a and c focus

on the cases where species thrive), and when *A. marina* was in sympatry with *A. defodiens* (e.g. reached the infralittoral level as shown on Figs. 11 and 13 d), high abundances of *A. marina* (over 6000 individuals) on potentially higher surface of the infralittoral shore (with lower bathymetry level reached) slightly negatively impacted the abundance of *A. defodiens* (Fig 13).

3.5.5. Size distribution and size at puberty

Inter-individual variability allowed for individuals of the same age to reach different sizes, leading to the presence of cohorts of varying sizes (Fig. 14). It also lead to varying sizes at puberty for each individuals in between populations and within one population (Fig. 15).

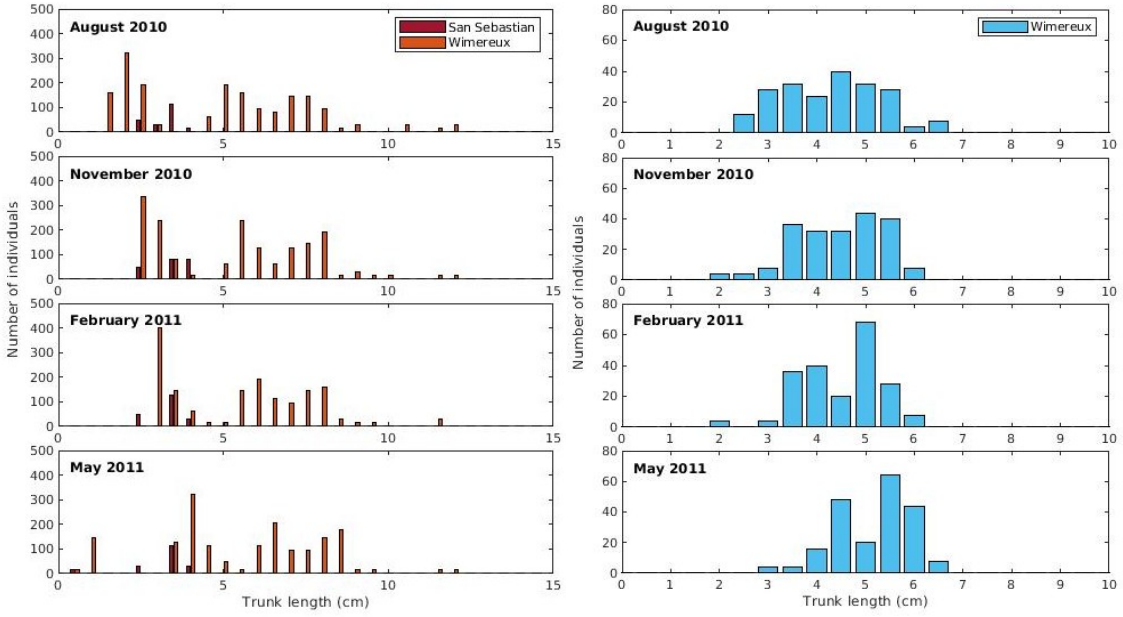

(a) (b)

Figure 14: Size distribution of the *A. marina*'s (a) and *A. defodiens*' (b) populations simulated by the DEB-IBM model in San Sebastian (dark red) and Wimereux (light orange and light blue) in August 2010, November 2010, February 2011 and May 2011.

For *A. marina*, size distributions at Wx and at SS appeared different, with individuals reaching up to 12 cm (trunk length) at Wx and less than 5 cm at SS (Fig. 14 a). Age cohorts at SS were extremely difficult to distinguish probably linked to a low growth rate, whilst age cohorts for ages 0+ (under 1 year old, 2 $\pm$ 0.5 cm in August 2010) and 1+ (under 2 years old, 3 to 4 $\pm$ 0.5 cm between November 2010 and May 2011) could clearly be identified at Wx, recruitment (e.g. the arrival of smaller individuals) happening between April-May and August (Fig. 14 a). Puberty was reached between 2.8 and 3 cm at Wx and between 2.1 and 2.9 cm at SS (Fig. 15).

For *A. defodiens*, sizes at Wx ranged from 2 to 7 cm in trunk length (Fig. 14 b). Age cohorts could not be clearly identified but it appeared that shore colonisation by young adults happened rather during autumn and winter, smaller individuals being present only in November and February (Fig. 14 b). At this site, puberty was reached between 1.4 and 1.5 cm (Fig. 15).

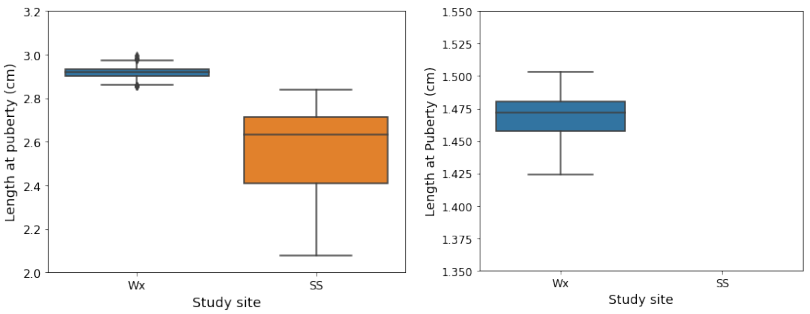

(a) (b)

Figure 15: Boxplot distributions in length at puberty of *A. marina* (a) and *A. defodiens* (b) populations simulated by the DEB-IBM model in San Sebastian (SS, orange) and Wimereux (Wx, blue).

4. Discussion

In August 2023, only 47 research articles out of the 5138 DEB-related research articles accessible in Web of Science (www.webofscience.com) dealt with DEB-IBMs, allowing the upscaling from individual to population levels. Among these, upscaling was achieved through generation of new individuals based on reproduction and through mortality. Combining these processes with variability of model parameters, and mobility and habitat preferences appeared even less common. In this study, the population dynamics, biological traits and shore distribution of two engineer polychaete species were mechanistically modelled in the North-East Atlantic along a latitudinal gradient using a newly developed fine-scale spatially-explicit DEB-IBM considering all these processes. The model allowed both comparison of mean biological traits among sites over a large range of environmental conditions and fine scale exploration of the on-shore mechanisms behind these macroscopic discrepancies. This kind of approach appears essential to provide a better understanding of marine populations, and potentially further community and ecosystem responses to small-scale (such as local shore fisheries) and large-scale (changing environmental conditions) human impact on the environment.

4.1. Main results

4.1.1. Empirical validation of the DEB-IBM

Our model's predictions of latitudinal distribution of population biological traits, of the impact of environmental forcings and of on-shore population processes and dynamics appeared in accordance with the majority of the body of literature existing about both species and was considered as an empirical qualitative validation of the DEB-IBM.

Predictions of the environmental scenarios . While environmental parameters displayed opposite trends, with overall northern regions displaying lower SST and higher chl-a concentration compared to southern regions displaying higher SST and lower chl-a concentration, the lower value of one did not compensate a higher value of the other. Indeed, SST latitudinal changes between sites did not impact greatly populations dynamics while higher concentrations of chl-a induced at the

same time higher maximum length, reproductive output and abundance. The idea that currently temperature is generally not a limiting factor for *A. marina* is in accordance with first De Cubber et al. (2020), who showed that shore migrations of lugworms are more likely to be linked with food concentration rather than temperature constraints, and second, with Wethey and Woodin (2022), who represented *A. marina*'s current area of distribution following extreme temperatures along most of the European Atlantic coasts.

Predictions of the latitudinal responses. A. marina's observations have been made from Portugal to Norway (Cadman and Nelson-Smith, 1993; De Cubber et al., 2018; Luttikhuizen and Dekker, 2010; Pires et al., 2015; Watson and Bentley, 1997) and are in accordance with our predictions of the species' latitudinal distribution. Predictions of *A. defodiens*'s latitudinal distribution also coincide with observations of the species made in Wales, the Eastern English Channel, the North Sea as well as in one lagoon of Portugal (Cadman and Nelson-Smith, 1993; De Cubber et al., 2018; Luttikhuizen and Dekker, 2010; Pires et al., 2015; Watson and Bentley, 1997). As it seems that population crashes for the species are linked to low levels of chl-a associated to high values of SST, the species might have thrived in Portugal, where it has been introduced, due to the high values of chl-a observed within the lagoon (close to sites 23 and 24 studied here).

Population-level processes. The DEB-IBM developed here considers most of the reviewed physiological (growth, reproduction and development) and behavioural mechanisms (density-dependant recruitment and foreshore migration and length-dependent foreshore migration) involved in *A. marina* and *A. defodiens*' populations dynamics and their relation to environmental parameters (De Cubber et al., 2018; 2019; 2020; Flach and Beukema, 1994; Reise et al., 2001; Watson et al, 2000). Some processes yet not fully described such as metabolic processes for *A. defodiens*, inter-individual variability in metabolic processes for both species, universal spawning thresholds for *A. marina* and mortality rates were added either based on novel experimental data (for *A. defodiens*), or on the literature, using available data. At a local scale, our results reproduce the trends obtained on the field in previous studies in terms of spawning and recruitment periods, zonation on the shore levels, shore migration and size distribution for *A. marina* (De Cubber et al., 2018;2020; Reise et al., 2001; Watson, 2000). Indeed, in our DEB-IBM, the reproduction period happens from late summer to mid autumn for *A. marina* as recorded by several authors (De Cubber et al., 2018; Watson et al, 2000), the recruitment period mostly occurs in late spring with a smoother pike (De Cubber et al., 2020; Reise et al., 2001), and an effect of adult shore density was shown on recruitment, as described by Flach and Beukema (1994). Recruitment indeed happens on the higher shore, where juveniles migrate down the shore while growing as previously described (De Cubber et al., 2020; Reise et al., 2001). Finally, simulated *A. marina*'s population size structure displayed similar patterns than those previously recorded at Wx in terms of mean size at age (around 4 cm for 1 year-old individuals in May, see De Cubber et al., 2020) and of coefficient of variation around

the mean size (10 to 20%, see De Cubber et al., 2020).

4.1.2. Underlying mechanisms

Density-dependant dynamics. Inter and intra-specific density-dependant interactions (competition) emerged from our model model properties. They could be observed only in the most favourable environmental conditions. Intra-specific density dependant recruitment for *A. marina* has been documented in the past in the Wadden Sea (Reise et al., 2001; Flach and Beukema, 1994), whilst competition between *A. defodiens* and *A. marina*, although predicted by our model, has not yet been studied to our knowledge. Indeed, mean population abundances of *A. defodiens* appear partly dependent on the abundance of *A. marina* at the lower shore under favourable environmental conditions. Such competition should be further studied to validate this aspect in our model, or to improve it in future versions. Different reasons could explain this competition, among which the competition for space (the smaller galleries being destroyed by larger individuals), for food and for oxygen, or a combination of these. The fact that species live or not in sympatry (Cadman, 1997) seems related to their ability to survive and thrive in a given environment. Low chl-a concentrations will be related to the absence of *A. defodiens* and the presence of rare *A. marina* individuals, while high chl-a concentrations will be related to the presence of both *A. defodiens* and *A. marina* on the lower shore.

Maturity size selection. Puberty was reached for larger sizes under favourable environmental conditions, and for lower sizes with a higher size variability at sites with less favourable environmental conditions, thus selecting individuals with a higher κ parameter in the first case and a smaller one in the second case. This could mean either that a selection of individuals reaching maturity early happens at sites with poor environmental conditions, or that under favourable environmental conditions, meaning high abundances, and thus higher intra-specific competition, these individuals do not manage to thrive and die early. The exact mechanism for this selection should be further studied in the future. In all cases if the site produces the majority of larvae that will recruit there, this could lead to differentiated populations displaying slightly different DEB parameters (such as a smaller κ).

Tipping points. Two types of tipping points, that "lead to abrupt and possibly irreversible shifts between alternative ecosystem states" (Dakos et al., 2019) could be detected and will be worth studying in the future. First, the one type leading to *A. defodiens*' population crash, that seemed linked to the temporal evolution of environmental forcings and their combination. Unless populations did not survive from the beginning, they appeared quite unpredictable in some cases where the population abundance was high and decreased abruptly. Second, the tipping point leading from a *A. marina*' population that displays the typical recruitment-spawning pattern and where the population is renewed and stable through time to a population with a really low number of individuals, and rare spawning and recruitment event. Although related to poor chl-a conditions,

this latter tipping point might also occur in cases where mortality is high due to harvesting (Olive, 1993), and where recruitment is low due to poor quality of the surrounding subtidal temporary habitats of larvae (De Cubber et al., 2018).

4.2. Limitations

4.2.1. Knowledge on A. defodiens*' biology*

The combination of the estimation of the energy maturation threshold for puberty, E_H^p, which is approximately 10 times lower for *A. defodiens* than for *A. marina*, and of a lower κ seems in accordance with biological observations of the two species (Table 2). Indeed, it is likely that *A. defodiens* invests indeed more energy in reproduction than *A. marina* with for instance 4000 oocytes per day for a black lugworm of 10 cm (this study) against 1000 oocytes per day for the lugworm *A. marina* of the same size (De Cubber et al. 2020), or reaches puberty (which is equivalent to age at first maturity in DEB vocabulary) earlier, as observations of gamete production were made in *A. defodiens* individuals much smaller (1.5 cm TLw; Gaudron unpublished) than what has been observed for *A. marina* (2.5 cm TLw; De Cubber et al., 2018, Table 2). However, maximum trunk length for *A. defodiens* might be higher as we based this value in the calibration process on data collected at sites 17, 18 ,19 and 20 (Sup. Mat. 4 and 6) where the species does not reach the highest maximum length value (Sup. Mat. 6)

4.2.2. Pelagic and benthic subtidal part of the life cycle

Little is known regarding the subtidal part of the life cycle of both species. As a consequence, we did not consider larval dispersal and survival, nor the presence or the absence of temporary subtidal settlement habitats for larvae, which might impact recruitment success (Lewin, 1986; De Cubber et al., 2018; 2019). This would require additional data as well as a better understanding of these aspects on the lugworm's lifecycle and on potential subtidal habitats. However this could be implemented in the future through the coupling of the DEB-IBM with biophysical model combining a model of physical circulation (MARS-3D model developed within the English Channel, see Ayata et al., 2009) and a larval transport model based on biological parameters such as the date of spawning, the number of emitted larvae, and the pelagic larval dispersal duration (e.g. time spent in the water column) (Failletaz, 2015). DEB models could provide the biological parameters needed to implement the larval dispersal model. Such a model could then allow to understand the populations' connectivity in the area (identifying the possible sources and sinks of propagules for example) and thus give valuable information for the conservation of the species. Populations genetics through the study of the gene fluxes could be combined with this approach (Hedgecock et al., 2007; Wright 1931). As an example, as abundances at some sites declined due to a lack of self recruitment in the current study, it would be interesting to study whether these sites can constantly be 'refilled' by individuals coming from other locations.

4.2.3. Regional adaptations

In our study, the DEB parameters of the two species do not vary geographically and the changes in the populations' simulated traits are due to differences in the environmental scenarios considered along the latitudinal gradient. Other DEB studies along environmental gradients have tested the possibility of variations in some DEB parameters across biogeographic regions. For example, Huret et al. (2018) did a regional calibration of one parameter (the maximum assimilation rate) to get better fit of growth trajectories and this may suggest a genetic adaptation. However, these authors acknowledge that an effect of food availability in quantity and quality could be not completely discarded. Further, a covariation with some other DEB parameters can be reasonably expected. Some clues seem to point out that genetic adaptation might occur for some populations of *A. marina* as well. Indeed, Schröer et al. (2009) studied the digging activity and the respiration rate for a range of temperatures (0°C to 22°C) of individuals of the species originated from three different regions (Atlantic, North Sea and White Sea) and showed that individuals from different regions did not display the same digging response to temperature. This would involve a change in other DEB parameters (e.g. the specific somatic maintenance rate, the temperature-specific parameters). Adjustments of some or all DEB parameters in-between regions could be investigated further to sub-populations of the species rather than to the whole data set but this will require collection of genetic data and population dynamics at the same spatial scales.

4.2.4. Predators and competitors

The estimation of the IBM mortality parameter used in this study (Table 2) could also be improved as it has only been fitted for one site among the 28 investigated and it does not dissociate death linked to ageing, predation, competition with other species or by harvesting pressure. As our main objective was first to assess the impact of environmental variables solely on populations' dynamics, and since we do not extrapolate results in terms of differences in mortality among sites, we believe that this should not impact our results interpretation beyond reason. However, in further studies, depending on the objectives that are aimed at, this aspect should be improved, as predation can lead to varying levels of mortality depending on the predator's density (Hastings, 2013), possibly leading to varying mortality rates among sites and according to time. Indeed, changes in predators' populations such as the sole (flat fish, De Vlas, 1979) are already reported (Van de Wolfshaar et al., 2021). Then et al. (2015) recommended to use the formula $\dot{m} = 4.899.t_{max}^{-0.916}$ to estimate fish mortality with $\dot{m}$ the natural mortality rate (year^{-1}) and t_{max} the maximum age (year). This leads to a daily mortality rate of 0.0026 d^{-1} for *A. marina* considering $t_{max} = 6$ years (De Cubber et al., 2020), which is 3.25 times higher than what has been estimated in this study (Table 2). This could be linked to phylogenetic (invertebrate vs fish) and lifestyle (mainly hidden in the sediment vs open water swimming) differences between species. Competition between lugworms and other species such as the eelgrass *Zostera noltii* or tube building polychaetes such as *Lanice conchilega* have already been reported by several authors (Kosche, 2007; Volkenborn

and Reise, 2007) and this could indeed impact their population dynamics.

4.2.5. Environmental variables

SST and chl-a values were extracted from 1 grid cell of respectively 4 and 1 km^2 only at sites where the species presence have been recorded. It could be interesting to compare our 1 cell environmental forcings to to the average of 9 cells to test our environmental data's robustness, although it would mean losing resolution. Other sites along the coast could also be considered in future studies. Of course, SST is different from sediment temperature, especially on the higher mediolittoral shore that remains emerged longer, and is used here as a proxy of the temperature experienced by lugworms (De Cubber et al., 2020). However, these differences were not found to impact greatly *A. marina*'s performances in terms of size and weight under current environmental conditions (De Cubber et al., 2020). Chl-a is also non homogeneous at the scale of the shore as well and is anyway a proxy of much more complex feeding mechanisms, but was found to be the best proxy available for the species (Chennu et al., 2015; De Cubber et al., 2020). Overall, as finer resolution observations at such a large scale with good quality data are not available elsewhere to our knowledge, we believe that the differences of mean values and their temporal variations in between sites give good ideas of latitudinal differences in between populations.

4.2.6. Model validation and sensitivity analysis

Quantitative validation for simulations made at Wx was not performed. However, all parameters of the model were calibrated at this site based on a large and diverse data set obtained from previous studies (De Cubber et al., 2018; 2019; 2020) and from extra experiments performed in this study (see respiration experiment for *A. defodiens*). At this site, the population dynamics simulated display the typical size distribution, migration (down-shore), recruitment (recruitment period and recruits location on the shore) and reproduction (spawning period) patterns described for the species by a number of authors (among which, De Cubber et al., 2018; 2019; 2020; Flach and Beukema, 1994; Reise et al., 2001; Watson et al, 2000). Overall, we consider that these comparisons are qualitative validation of our model. To validate the model quantitatively at this site and use it for management, new independent field sampling and laboratory work should be performed to test its reproducibility. Besides, as the idea of this study is rather a comparison of the model's behaviour in between contrasted environmental conditions than a very accurate site-specific prediction on population traits, we believe that our results are still interesting and overall reliable. In the prospect of using this model as a tool for management, a sensitivity analysis on the model's parameters should also be implemented (Matyja, 2023).

4.3. Model prospects

4.3.1. Fisheries

In order to prevent the two species over-exploitation (Blake, 1979; Olive, 1993; De Cubber et al., 2018), potentially leading to changes in size and age structure, abundance and distribution of local populations, several authors have emphasised the need for managing polychaete species

(Watson et al., 2017; Xenarios, 2018). These management measures aim at limiting the overall mortality, or the mortality of specific individuals in the population, based on its features (FAO, 2012). Such measures have been implemented in some areas, generally consisting in licensing for commercial harvesters and in maximum daily catches for recreational fishermen, with in rare cases (UK) local management strategies adapted to the stakes of the area (Cabral et al., 2019). The DEB-IBM developed in this study could be used by conservation managers as a tool to explore several management scenarios after validation procedure is performed. This could be done by adding a distinction between the fishery-related mortality rate from other mortality types, and potentially spatialising this new mortality rate and/or making it relative to the individuals size. For example, a size limit impact on the population structure and the TRO (depending on if the size limit exceeds the length at puberty or not) could be tested, as well as the impact of closing an area (the entire shore or only the higher shore as suggested by De Cubber et al., 2018) to fisheries (with a fisheries-related mortality set to zero in the considered area) on the overall population's dynamics. Other management scenarios such as a closing season, the implementation of quotas, licenses or tool restrictions could also be explored.

4.3.2. Climate change and heat waves

Climate change can affect the distribution and population dynamics of marine organisms (Kearney et al., 2009; Thomas and Bacher, 2018). The Intergovernmental Panel on Climate Change predicted a warming of Sea-Surface Temperature of 1 to almost 5 °C by 2100 (IPCC, 2021). In this context, the DEB-IBM implemented in this study constitutes a powerful tool for predicting lugworms' responses to climate change in terms of populations dynamics, biological traits by using the projections in terms of SST and chl-a provided by the IPCC. However, due to the cascade of impacts that occur at the land–ocean interface, biogeochemical and hydrological models still struggle to provide accurate projections in terms of future time series for global coastal chl-a (Raimonet et al., 2018).

Although high temperatures did not appear in this study a major issue for lugworms' survival in comparison to low chl-a concentrations, marine heatwaves are likely to intensify in the next decades and have already been identified as a challenge for lugworms' species (Wethey and Woodin, 2022). We believe this issue could be addressed in our DEB-IBM considering the effect of oxygen content of the sediment on lugworm density and shore migration. Indeed, in this study, IBM parameters related to density (maximum local densities at different levels of the foreshore) were defined non-mechanistically according to what was reported in the literature (Table 2, De Cubber et al., 2018). An alternative method would be to consider the maximum carrying capacity of the shore in terms of the oxygen content within the sediment. Indeed, lugworms can remain within emerged sediments for periods exceeding 6 hours (Schöttler, 1989) leading to depletion of the surrounding oxygen or food that keep being consumed by individuals. When SST increases, the dissolved oxygen decreases (Aminot and Kerouel, 2004), leading to a potential decrease in lugworms density if thermal changes

are gradual, or to an increase in mortality if changes are sudden. In this case, the development of a DEB model accounting for low activity levels at emersion and high activity levels at immersion could be considered.

4.3.3. Bioturbation and impact on communities

Bioturbation by lugworms contributes to limit the evolution of sandy sediments to muddy sediments (Volkenborn et al., 2007). Indeed, in some areas, layers of 17 to 40 cm of the whole shores's sediment can be reworked annually by lugworms, depending on the size of lugworms, their density, and the period of the year (temperature and food effects on metabolism) (Cadée, 1976). The decline of lugworms' populations predicted by Wethey and Woodin (2022) in southern areas would thus lead to new bio-physical features of these shores. Given the mechanistic properties of our DEB-IBM, such decline in bioturbation could be quantified finely by adding a relation between lugworms size/weight and sand reworking volume according to temperature and food level obtained from laboratory experiments. Such knowledge could also give insights on the possible evolution of the whole associated bentho-pelagic community in a climate change context in areas where lugworms will be extending or decreasing. As an example, *A. marina* has been shown to impact negatively populations of *Zostera noltii* (Kosche, 2007) and to influence the local community compositions (Donadi et al., 2015). Its observed expansion in southern areas (Pires et al., 2015) might lead to shifts in the communities there. Indeed, Volkenborn and Reise (2007) showed significant differences in polychaete functional group composition in lugworm exclusion plots compared to control and ambient plots.

Apart from these prospects, the mechanistic nature of our DEB-IBM makes it easily adaptable to new questions from scientists and managers that might arise in the next decades. Besides, despite its complexity, the construction of the model around biological processes can make it understandable at least from a conceptual view to non-modelers such as conservation managers and could become a valuable tool in the next years to study the *A. marina* and *A. defodiens* population dynamics in a variety of situations.

Acknowledgements

We would like to thank L. Denis for the use of the system to carry the respiration experiments, and H. Loisel for his advice on our work. We are grateful to Europe (FEDER), the state and the Region Hauts-de-France for funding the experimental set up and field work, and the salaries of T. Lancelot (research assistant) and L. De Cubber (Post-doctoral fellowship) through the CPER MARCO 2015–2020.

References

Aminot, A., Kerouel, R., 2004. Hydrologie des écosystèmes marins; paramètres et analyses,628 Ifremer. ed.

Ayata, S.-D., Ellien, C., Dumas, F., Dubois, S., Thiébaut, É., 2009. Modelling larval dispersal and settlement of the reef-building polychaete *Sabellaria alveolata*: Role of hydroclimatic processes on the sustainability of biogenic reefs. Cont. Shelf Res. 29(13), 1605–1623. https://doi.org/10.1016/j.csr.2009.05.002

Bacher, C., Gangnery, A., 2006. Use of dynamic energy budget and individual based models to simulate the dynamics of cultivated oyster populations. J. Sea Res. 56, 140–155.

Batabyal, A.A., 1996. On some aspects of the management of a stochastically developing forest. Ecol. Model. 89: 67–72.

Beaudouin, R., Dias, V., Bonzom, J. M., Péry, A., 2012. Individual-based model of *Chironomus riparius* population dynamics over several generations to explore adaptation following exposure to uranium-spiked sediments. Ecotoxicology, 21(4), 1225–1239. https://doi.org/10.1007/s10646-012-0877-4

Blake, R.W., 1979. Exploitation of a natural population of *Arenicola marina* (L.) from the North-East Coast of England. J. Appl. Ecol. 16, 663–670. https://doi.org/ 10.2307/2402843

Cabral, S., Alves, A., Nuno, C., Pedro, F. E. C., Erica, S., João, C., Luís, C. D. F., Paula, C., João, C.-C., David, P., Ana, P., José Lino, C., 2019. Polychaete annelids as live bait in Portugal: harvesting activity in estuarine systems. Ocean Coast. Manag. https://doi.org/10.3389/conf.fmars.2016.04.00111

Cadée, G. C. 1976. Sediment reworking by *Arenicola marina* on tidal flats in the Dutch Wadden Sea. Netherlands J. Sea Res. 10(4), 440–460.

Cadman, P.S., Nelson-Smith, A., 1993. A new species of lugworm: *Arenicola defodiens* sp. nov. mar. biol. Ass. U.K 73, 213–223. https://doi.org/10.1017/S0025315 400032744

Cadman, P.S., 1997. Distribution of two species of lugworm (*Arenicola*) (Annelida: Polychaeta) in South Wales. J. Mar. Biol. Assoc. U.K. 77, 389–398. https://doi.org/10.1017/S0025315400071745

Caswell, H., 2001. Matrix Population Models: Construction, Analysis and Interpretation. Sunderland, Massachusetts: Sinauer Associates, Inc. Publishers, 2nd edition, 722.

Chennu, A., Volkenborn, N., De Beer, D., Wethey, D.S., Woodin, S.A., Polerecky, L., 2015. Effects of Bioadvection by *Arenicola marina* on Microphytobenthos in Permeable Sediments. PLoS One 10, e0134236.

Clarke, L.J., Hughes, K.M., Esteves, L.S., Herbert, R.J.H., Stillman, R.A., 2017. Intertidal invertebrate harvesting: a meta-analysis of impacts and recovery in an important waterbird prey resource. Mar. Ecol. Prog. Ser. 584, 229–244. https://doi. org/10.3354/meps12349

839 Coulson, T., 2012. Integral projections models, their construction and use in posing hypothe-
840 ses in ecology. Oikos 121: 1337–1350.

841 Dakos, V., Matthews, B., Hendry, A. P., Levine, J., Loeuille, N., Norberg, J., Nosil, P.,
842 Scheffer, M., De Meester, L., 2019. Ecosystem tipping points in an evolving world. Nat.
843 Ecol. Evol., 3(3), 355–362. https://doi.org/10.1038/s41559-019-0797-2

844 David, V., Joachim, S., Tebby, C., Porcher, J. M., Beaudouin, R., 2019. Modelling population
845 dynamics in mesocosms using an individual-based model coupled to a bioenergetics model.
846 Ecol. Model., 398(March), 55–66. https://doi.org/10.1016/j.ecolmodel.2019.02.008

847 Davis, A. J., Jenkinson, L. S., Lawton, J. H., Shorrocks, B., Wood, S., 1998. Making mistakes
848 when predicting shifts in species range in response to global warming. Nature 391, 783–786.
849 https://doi.org/10.1038/35842

850 De Angelis, D. L., Grimm, V., 2014. Individual-based models in ecology after four decades.
851 F1000 Prime Reports, 6–39. https://doi.org/10.12703/P6-39

852 De Cubber, L., Lefebvre, S., Fisseau, C., Cornille, V., Gaudron, S.M., 2018. Linking life-
853 history traits, spatial distribution and abundance of two species of lugworms to bait collection:
854 A case study for sustainable management plan. Mar. Environ. Res. https://doi.org/10.1016
855 /j.marenvres.2018.07.009

856 De Cubber, L., Lefebvre, S., Lancelot, T., Denis, L., Gaudron, S. M., 2019. Annelid poly-
857 chaetes experience metabolic acceleration as other Lophotrochozoans: Inferences on the life
858 cycle of *Arenicola marina* with a Dynamic Energy Budget model. Ecol. Model. 410, 108773.
859 https://doi.org/10.1016/j.ecolmodel.2019. 108773

860 De Cubber, L., Lefebvre, S., Lancelot, T., Duong, G., Gaudron, S. M, 2020. Investigating
861 down-shore migration effects on individual growth and reproduction of the ecosystem engineer
862 *Arenicola marina*. J. Mar. Sys. 211(5): 103420. https://doi.org/10.1016/j.jmarsys.2020.
863 103420

864 De Vlas, J., 1979. Secondary production by tail regeneration in a tidal flat population of
865 lugworms (*Arenicola marina*), cropped by flatfish. Netherlands J. Sea Res. 13, 362–393.
866 https://doi.org/10.1016/0077-7579(79)90012-7

867 Donadi, S., van der Heide, T., Piersma, T., van der Zee, E.M., Weerman, E.J., van de Koppel,
868 J., Olff, H., Devine, C., Hernawan, U.E., Boers, M., Planthof, L., Klemens Eriksson, B., 2015.
869 Multi-scale habitat modification by coexisting ecosystem engineers drives spatial separation
870 of macrobenthic functional groups. Oikos 124, 1502–1510. https://doi.org/10.1111/oik.02100

Ellien, C., Thiébaut, E., Dumas, F., Salomon, J. C., Nival, P. (2004). A modelling study of the respective role of hydrodynamic processes and larval mortality on larval dispersal and recruitment of benthic invertebrates: Example of *Pectinaria koreni* (Annelida: Polychaeta) in the Bay of Seine (English Channel). J. Plankton Res. 26(2), 117–132. https://doi.org/10.1093/plankt/fbh018

Failletaz, R., 2015. Estimation des capacités comportementales des larves de poissons et leurs implications pour la phase larvaire. Université Pierre et Marie Curie - Paris 6. Ph D Thesis.

FAO, 2012. Recreational fisheries, FAO Technical Guidelines for Responsible Fisheries. Rome.

Farke, H., Berghuis, E.M., 1979a. Spawning, larval development and migration of *Arenicola marina* under field conditions in the western Wadden sea. Netherlands J. Sea Res. 13, 529–535.

Farke, H., Berghuis, E.M., 1979b. Spawning, larval development and migration behaviour of *Arenicola marina* in the laboratory. Netherlands J. Sea Res. 13, 512–528.

Flach, E.C., Beukema, J.J., 1994. Density-governing mechanisms in populations of the lugworm *Arenicola marina* on tidal flats. Mar. Ecol. Prog. Ser. 115, 139–150. https://doi.org/10.3354/meps115139

Grimm, V., 1999. Ten years of individual-based modelling in ecology: what have we learned and what could we learn in the future? Ecol. Model. 115: 129–148

Grimm, V., Railsback, S. F., Vincenot, C. E., Berger, U., Gallagher, C., Deangelis, D. L., Edmonds, B., Ge, J., Giske, J., Groeneveld, J., Johnston, A. S. A., Milles, A., Nabe-Nielsen, J., Polhill, J. G., Radchuk, V., Rohwäder, M. S., Stillman, R. A., Thiele, J. C., Ayllón, D., 2020. The ODD protocol for describing agent-based and other simulation models: A second update to improve clarity, replication, and structural realism. Jasss, 23(2). https://doi.org/10.18564/jasss.4259

Haberle, I., Bavčević, L., Tin Klanjscek, T., 2023. Fish condition as an indicator of stock status: Insights from condition index in a food-limiting environment. Fish. Fish. 24(4) https://doi.org/10.1111/faf.12744

Halpern, B. S., Frazier, M., Potapenko, J., Casey, K. S., Koenig, K., Longo, C., Lowndes, J. S., Rockwood, R. C., Selig, E. R., Selkoe, K. A., Walbridge, S., 2015. Spatial and temporal changes in cumulative human impacts on the world's ocean. Nature Communications, 6, 7615. https://doi.org/10.1038/ncomms8615

Harley, C. D. G., Hughes, A. R., Hultgren, K. M., Miner, B. G., Sorte, C. J. B., Thornber, C. S., Rodriguez, L. F., Tomanek, L., Williams, S. L., 2006. The impacts of climate change in coastal marine systems. Ecol. Lett., 9(2), 228–241. https://doi.org/10.1111/j.1461-0248.2005.00871.x

Hastings, A., 2013. Population Dynamics. Encyclopedia of Biodiversity: Second Edition, 6, 175–181. https://doi.org/10.1016/B978-0-12-384719-5.00115-5

Hedgecock, D., Barber, P., Edmands, S., 2007. Genetic approaches to measuring connectivity. Oceanography, 20:70–79

Holmes, E.E., Lewis, M.A., Banks, J.E., Veit, R.R., 1994. Partial differential equations in ecology: spatial interactions and population dynamics. Ecology 75: 17–29.

Howie, D., 1984. The reproductive biology of the lugworm, *Arenicola marina* L. Fortschritte Der Zoologie, 29, 247–263.

Huret, M., Tsiaras, K., Daewel, U., Skogen, M. D., Gatti, P., Petitgas, P., Somarakis, S., 2018. Variation in life-history traits of European anchovy along a latitudinal gradient: A bioenergetics modelling approach. MEPS, 2018(May). https://doi.org/10.3354/meps12574

Huston, M.A., De Angelis, D.L., Post, W.M., 1988. New computer models unify ecological theory. BioSci. 38: 682–691.

IPCC, 2021: Climate Change 2021: The Physical Science Basis. Contribution of Working Group I to the Sixth Assessment Report of the Intergovernmental Panel on Climate Change[Masson-Delmotte, V., P. Zhai, A. Pirani, S.L. Connors, C. Péan, S. Berger, N. Caud, Y. Chen, L. Goldfarb, M.I. Gomis, M. Huang, K. Leitzell, E. Lonnoy, J.B.R. Matthews, T.K. Maycock, T. Waterfield, O. Yelekçi, R. Yu, and B. Zhou (eds.)]. Cambridge University Press, Cambridge, United Kingdom and New York, NY, USA, doi:10.1017/9781009157896.

Kearney, M., Shine, R., Porter, W.P., 2009. The potential for behavioral thermoregulation to buffer ‘“ cold-blooded ”’ animals against climate warming. PNAS 106, 3835–3840.

Kearney, M., Simpson, S.J., Raubenheimer, D., Helmuth, B., 2010. Modelling the ecological niche from functional traits. Philos. Trans. R. Soc. Lond. B. Biol. Sci. 365, 3469–3483. https://doi.org/10.1098/rstb.2010.0034

Koch, J., De Schamphelaere, K. A. C. (2020). Estimating inter-individual variability of dynamic energy budget model parameters for the copepod *Nitocra spinipes* from existing life-history data. Ecol. Model. 431, 109091. https://doi.org/10.1016/j.ecolmodel.2020.109091

Kooijman, S. A. L. M., 2014. Metabolic acceleration in animal ontogeny: An evolutionary perspective. J. Sea Res., 94, 128–137. https://doi.org/10.1016/j.seares.2014.06.005

Kooijman, S.A.L.M., 2010. Dynamic energy budget theory for metabolic organisation. Cambridge University Press.

Kosche, K., 2007. The influence of current velocity, tidal height and the lugworm *Arenicola marina* on two species of seagrass, *Zostera marina* L. and *Z. noltii* Hornemann. Bremen University.

Kristensen, E., 2001. Impact of polychaetes (*Nereis* spp. and *Arenicola marina*) on carbon biogeochemistry in coastal marine sediments. Geochem. Trans. 2, 92–103. https://doi.org/10.1186/1467-4866-2-92

Lewin, R. (1986). Supply-side ecology. Science, 234:25–27.

Luttikhuizen, P.C., Dekker, R., 2010. Pseudo-cryptic species *Arenicola defodiens* and *Arenicola marina* (Polychaeta: Arenicolidae) in Wadden Sea, North Sea and Skagerrak: Morphological and molecular variation. J. Sea Res. 63, 17–23. https://doi.org/10.1016/j.seares.2009.09.001

Malishev, M., Bull, M.C., Kearney, M.R., 2017. An individual-based model of ectotherm movement integrating metabolic and microclimatic constraints. Methods Ecol. Evol. 9, 472–489. https://doi.org/10.1111/ijlh.12426

Mangano, M. C., Giacoletti, A., Sarà, G., 2019. Dynamic Energy Budget provides mechanistic derived quantities to implement the ecosystem based management approach. Journal of Sea Research, 143, 272–279. https://doi.org/10.1016/j.seares.2018.05.009

Mangano, M. C., Mieszkowska, N., Helmuth, B., Domingos, T., Sousa, T., Baiamonte, G., Bazan, G., Cuttitta, A., Fiorentino, F., Giacoletti, A., Johnson, M., Lucido, G. D., Triantafyllou, G., 2020. Moving Toward a Strategy for Addressing Climate Displacement of Marine Resources: A Proof-of-Concept. Frontiers in Marine Science, 7, 1–16. https://doi.org/10.3389/fmars.2020.00408

Marques, G. M., Augustine, S., Lika, K., Pecquerie, L., Domingos, T., Kooijman, S. A. L. M., 2018. The AmP project: Comparing species on the basis of dynamic energy budget parameters. PLoS Comput. Biol., 14(5), 1–23. https://doi.org/10.1371/journal.pcbi.1006100

Martin, B.T., Zimmer, E.I., Grimm, V., Jager, T., 2012. Dynamic Energy Budget theory meets individual-based modelling: A generic and accessible implementation. Methods Ecol. Evol. 3, 445–449. https://doi.org/10.1111/j.2041-210X.2011.00168 .x

Matyja, K., 2023. Standard dynamic energy budget model parameter sensitivity. Ecol. Model. 478:110304. https://doi.org/10.1016/j.ecolmodel.2023.110304.

Newell, G.E., 1949. The later larval life of *Arenicola marina*. J. Mar. Biol. Assoc. UK 28, 635–639. https://doi.org/https://doi.org/10.1017/S0025315400023456

Newell, G.E., 1948. A contribution to our knowledge of the life history of *Arenicola marina* L. J. Mar. Biol. Assoc. UK 27, 554–580. https://doi.org/10.1017/S0025315 400056022

Olive, P.J.W., 1993. Management of the exploitation of the lugworm *Arenicola marina* and the ragworm *Nereis virens* (Polychaeta) in conservation areas. Aquat. Conserv. Mar. Freshw. Ecosyst. 3, 1–24. https://doi.org/10.1002/aqc.3270030102

Pethybridge, H., Roos, D., Loizeau, V., Pecquerie, L., Bacher, C., 2013. Responses of European anchovy vital rates and population growth to environmental fluctuations : An individual-based modeling approach. Ecol. Modell. 250, 370–383. https://doi.org/10.1016/j.ecolmodel.2012.11.017

Picard, N., Liang, J., 2014. Matrix models for size-structured populations: Unrealistic fast growth or simply diffusion? PLoS ONE, 9(6). https://doi.org/10.1371/journal.pone.0098254

Pires, A., Martins, R., Magalhães, L., Soares, A., Figueira, E., Quintino, V., Rodrigues, A., Freitas, R., 2015. Expansion of lugworms towards southern European habitats and their identification using combined ecological, morphological and genetic approaches. Mar. Ecol. Prog. Ser. 533, 177–190. https://doi.org/10.3354/mep s11315

Raimonet, M., Thieu, V., Silvestre, M., Oudin, L., Rabouille, C., Vautard, R., Garnier, J., 2018. Landward perspective of coastal eutrophication potential under future climate change: The Seine River case (France). Front. Mar. Sci., 5, 1–16. https://doi.org/10.3389/fmars.2018.00136

Reise, K., 1985. Tidal flat ecology - An experimental approach to species interactions, Ecological Studies 54. 316 pp.

Reise, K., Simon, M., Herre, E., 2001. Density-dependent recruitment after winter disturbance on tidal flats by the lugworm *Arenicola marine*. Helgol. Mar. Res. 55, 161–165. https://doi.org/10.1007/s101520100076

Ritter, F. E., Schoelles, M. J., Quigley, K. S., 2011. Determining the number of simulation runs: treating simulations as theories by not sampling their behavior. In Human-in-the-Loop Simulations (pp. 97–116). https://doi.org/10.1007/978-0-85729-883-6

Schöttler, U., 1989. Anaerobic metabolism in the lugworm *Arenicola marina* during low tide: the influence of developing reproductive cells. Comp. Biochem. Physiol. , 92A(I), 1–7.

Schröer, M., Wittmann, A. C., Grüner, N., Steeger, H. U., Bock, C., Paul, R., Pörtner, H. O., 2009. Oxygen limited thermal tolerance and performance in the lugworm Arenicola marina: A latitudinal comparison. J. Exp. Mar. Biol. Ecol., 372(1–2), 22–30. https://doi.org/10.1016/j.jembe.2009.02.001

Senga Green, D., Boots, B., Sigwart, J., Jiang, S., Rocha, C., 2016. Effects of conventional and biodegradable microplastics on a marine ecosystem engineer (*Arenicola marina*) and sediment nutrient cycling. Environ. Pollut. 208, 426–434. https://doi.org/10.1016/j.envpol.2015.10.010

Then, A. Y., Hoenig, J. M., Hall, N. G., Hewitt, D. A., 2015. Evaluating the predictive performance of empirical estimators of natural mortality rate using information on over 200 fish species. CES J. Mar. Sci. 72(1), 82–92. https://doi.org/10.2307/4451538

Thomas, Y., Bacher, C., 2018. Assessing the sensitivity of bivalve populations to global warming using an individual-based modelling approach. Glob. Chang. Biol. 24, 4581–4597. https://doi.org/10.1111/gcb.14402

Thomas, Y., Razafimahefa, N. R., Ménesguen, A., Bacher, C., 2020. Multi-scale interaction processes modulate the population response of a benthic species to global warming. Ecol. Mod., 436 (March), 109295. https://doi.org/10.1016/j.ecolmodel.2020.109295

Van De Wolfshaar, K. E., Barbut, L., Lacroix, G., 2021. From spawning to first-year recruitment: the fate of juvenile sole growth and survival under future climate conditions in the North Sea. ICES J. Mar. Sci. https://doi.org/10.1093/icesjms/fsab025

Violle, C., Navas, M.-L., Vile, D., Kazakou, E., Fortunel, C., Hummel, I., Garnier, E., 2007. Let the concept of trait be functional!. Oikos 116, 882–892. https://doi.org/10.1111/j.2007.0030-1299.15559.x.

Volkenborn, N., 2005. Ecosystem engineering in intertidal sand by the lugworm *Arenicola marina*. University of Bremen. Ph D Thesis.

Volkenborn, N., Reise, K., 2007. Effects of *Arenicola marina* on polychaete functional diversity revealed by large-scale experimental lugworm exclusion. J. Sea Res. 57(1), 78–88. https://doi.org/10.1016/j.seares.2006.08.002

Watson, G. J., Bentley, M. G., 1997. Evidence for a coelomic maturation factor controlling oocyte maturation in the polychaete *Arenicola marina* (L). Invertebr. Reprod. Dev., 31(1–3), 297–305. https://doi.org/10.1080/07924259.1997.9672589

Watson, G.J., Cadman, P.S., Paterson, L.A., Bentley, M.G., Auckland, M.F., 1998. Control of oocyte maturation, sperm activation and spawning in two lugworm spec-ies: *Arenicola ma-*

rina and *A. defodiens*. Mar. Ecol. Prog. Ser. 175, 167–176. https://doi.org/10.3354/meps175167

Watson, G.J., Williams, M.E., Bentley, M.G., 2000. Can synchronous spawning be predicted from environmental parameters? A case study of the lugworm *Arenicola marina*. Mar. Biol. 136, 1003–1017.

Watson, G.J., Murray, J.M., Schaefer, M., Bonner, A., 2017. Bait worms: a valuable and important fishery with implications for fisheries and conservation management. Fish Fish. 18, 374–388. https://doi.org/10.1111/faf.12178

Wethey, D.S., Woodin, S. A., 2022. Climate change and *Arenicola marina*: Heat waves and the southern limit of an ecosystem engineer. Estuar. Coast. Shelf Sci. 276(15):108015 DOI: 10.1016/j.ecss.2022.108015

Wethey, D.S., Woodin, S.A., Hilbish, T.J., Jones, S.J., Lima, F.P., Brannock, P.M., 2011. Response of intertidal populations to climate: Effects of extreme events versus long term change. J. Exp. Mar. Biol. Ecol., 400(1–2), 132–144. https://doi.org/10.1016/j.jembe.2011.02.008

Wrede, A., Andresen, H., Asmus, R., Wiltshire, K. H., Brey, T., 2019. Macrofaunal irrigation traits enhance predictability of nutrient fluxes across the sediment-water interface. Marine Ecology Progress Series, 632(2004), 27–42. https://doi.org/10.3354/meps13165

Wright, S. 1931. Evolution in Mendelian populations. Genetics, 97, 97–159.

Xenarios, S., Queiroga, H., Lillebø, A., Aleixo, A., 2018. Introducing a regulatory policy framework of bait fishing in European Coastal Lagoons: The case of Ria de Aveiro in Portugal. Fishes 3, 2. https://doi.org/10.3390/fishes3010002

Yeakel, J. D., Pires, M. M., Aguiar, M. A. M. De, Donnell, J. L. O., Jr, P. R. G., Gravel, D., Gross, T., 2020. Diverse interactions and ecosystem engineering can stabilize community assembly. Nature Communications, 1–10. https://doi.org/10.1038/s41467-020-17164-x

Supplementary Material

Sup. Mat. 1 - Lifecycles and Dynamic Energy Budget

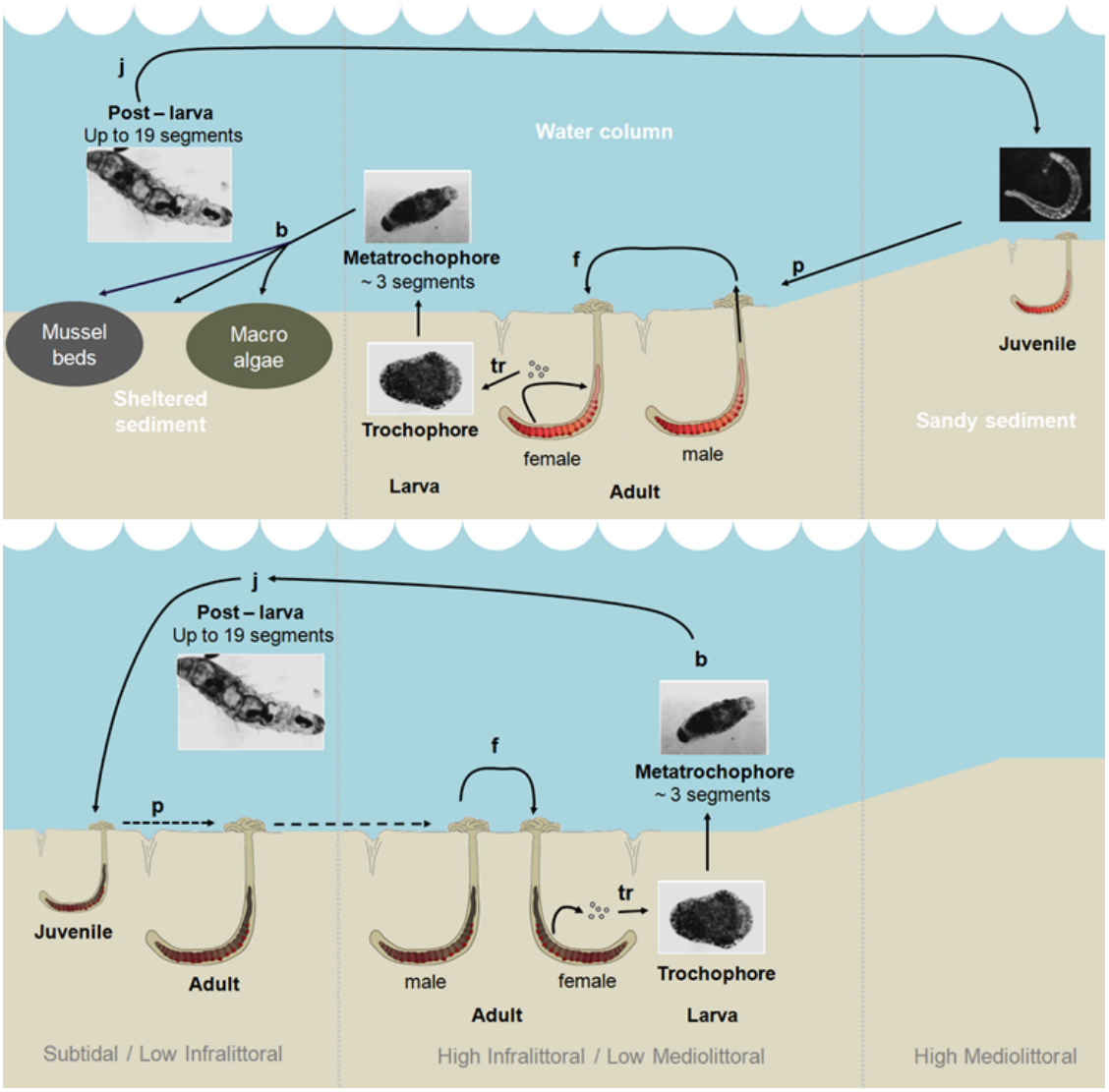

Lifecycle of *Arenicola marina* (above), hypothesis on the lifecycle of *A. defodiens* and associated habitats. Adapted from De Cubber et al. (2019), Farke and Berghuis (1979a, 1979b), Reise (1985) and Reise et al. (2001). f stands for fertilization; tr for when the trochophore larva appears; b for birth (e.g. first feeding, as described in the DEB theory); j for the end of metamorphosis; and p for puberty. Pictures of the different life stages of *A. marina* are taken from Farke and Berghuis (1979a).

Sup. Mat. 2 - Estimation of DEB parameters for A. defodiens

Sup. Mat. 2.1: Available data set for the parameter estimation of a DEB model for *Arenicola defodiens* and the associated prediction and relative error (RE) temperature, scaled functional response and reference.

Type of data	Data	Symbol	Value	Prediction (RE)	Unit	Temperature (°C)	f	References
Zero-variate	age at trochophore larva	a_{tr}	3	3 (0.00)	d	13	1	De Cubber unpublished
	age at metamorphosis	a_j	90	90.21 (0.00)	d	12	1	Farke and Berghuis (1979)
	egg diameter	L_0	0.015	0.015 (0.001)	cm	-	1	De Cubber et al. (2018)
	length of the trochophore larva	L_{tr}	0.014	0.014 (0.00)	cm	-	1	De Cubber unpublished
	trunk length at puberty	TL_p	1.5	1.5 (0.00)	cm	-	1	Gaudron unpublished
	maximum trunk length	TL_i	25	23.84 (0.05)	cm	-	1	This study
	maximum wet weight	Ww_i	60	62 (0.03)	g	-	1	This study
	wet weight of an egg	Ww_0	1.8 10^{-6}	1.8 10^{-6} (0.00)	g	-	1	De Cubber unpublished
Uni-variate	Length-Weight	TL-Ww	-	$g.cm^{-1}$	-	-	0.8	This study
	Oxygen consumption	Ww-O2	-	-	µmol $O2.h^{-1}$	10, 13, 16, 20, 24	0.8	This study
	Fecundity	TL-R	-	-	$oocytes.year^{-1}.cm^{-1}$	13	1	De Cubber unpublished

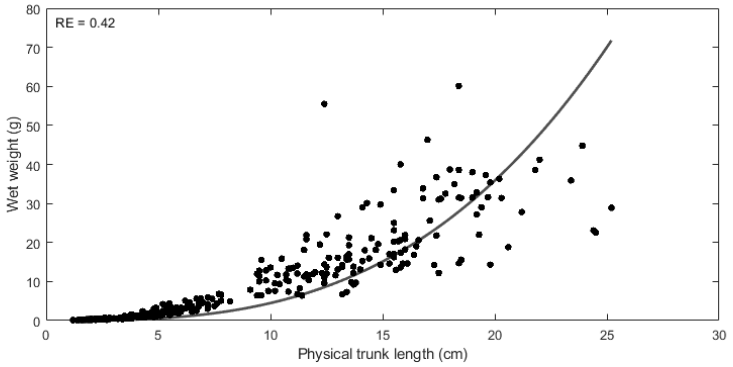

Sup. Mat. 2.2: Data (dots) and predictions (lines) of the wet weight as a function of trunk length for *Arenicola defodiens* individuals collected in the Eastern English Channel (France) using an abj-DEB model. The corresponding value of the shape coefficient is $\delta_M = 0.16$. RE stands for relative error.

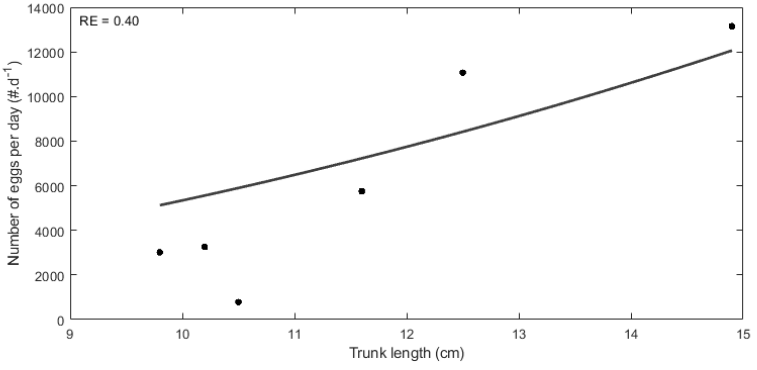

Sup. Mat. 2.3: Data (dots) and predictions (lines) of the number of oocytes produced per day as a function of trunk length for *Arenicola defodiens* individuals collected in the Eastern English Channel (France) using an abj-DEB model. RE stands for relative error.

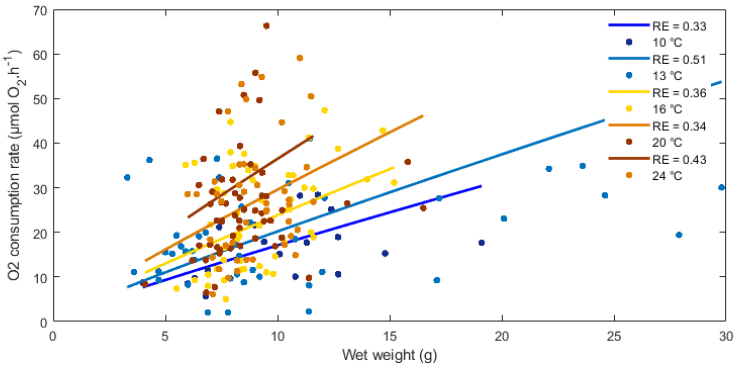

Sup. Mat 2.4: Data (dots) and predictions (lines) of the oxygen consumption of the abj-DEB model of *Arenicola defodiens* measured by the authors as a function of wet weight at five different temperatures (from blue to red: 10, 13, 16, 20 and 24°C). The respective relative errors from 10 to 24°C were 0.33, 0.51, 0.36, 0.34 and 0.43 with the abj-model.

Sup. Mat. 3 - Estimation of the Individual-Based Model parameters

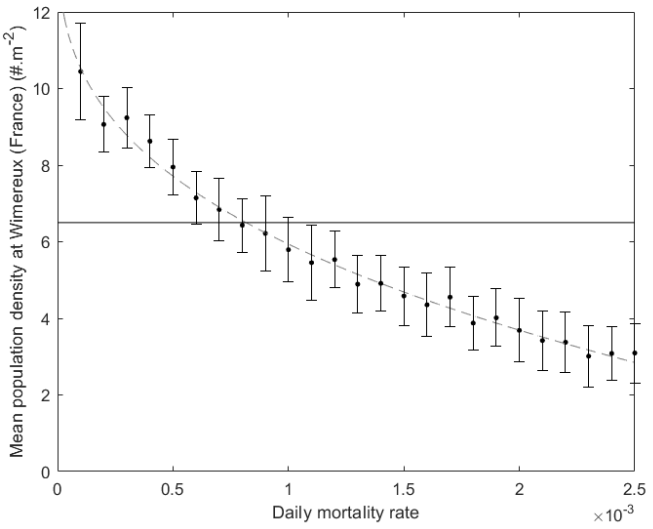

Sup. Mat. 3.1: Mean and sd population density of *A. marina* at Wimereux (Wx, Easter English Chanel, France) obtained with the IBM model according to various mortality rate values. The fitted model (dottend grey line) for the relation between the mean population density at the site and the daily mortality rate was (R^2: 0.99): $Density = 14.42 - 88.16.\dot{m}^{0.3389}$. The observed Mean population density at Wx is represented by the horizontal line.

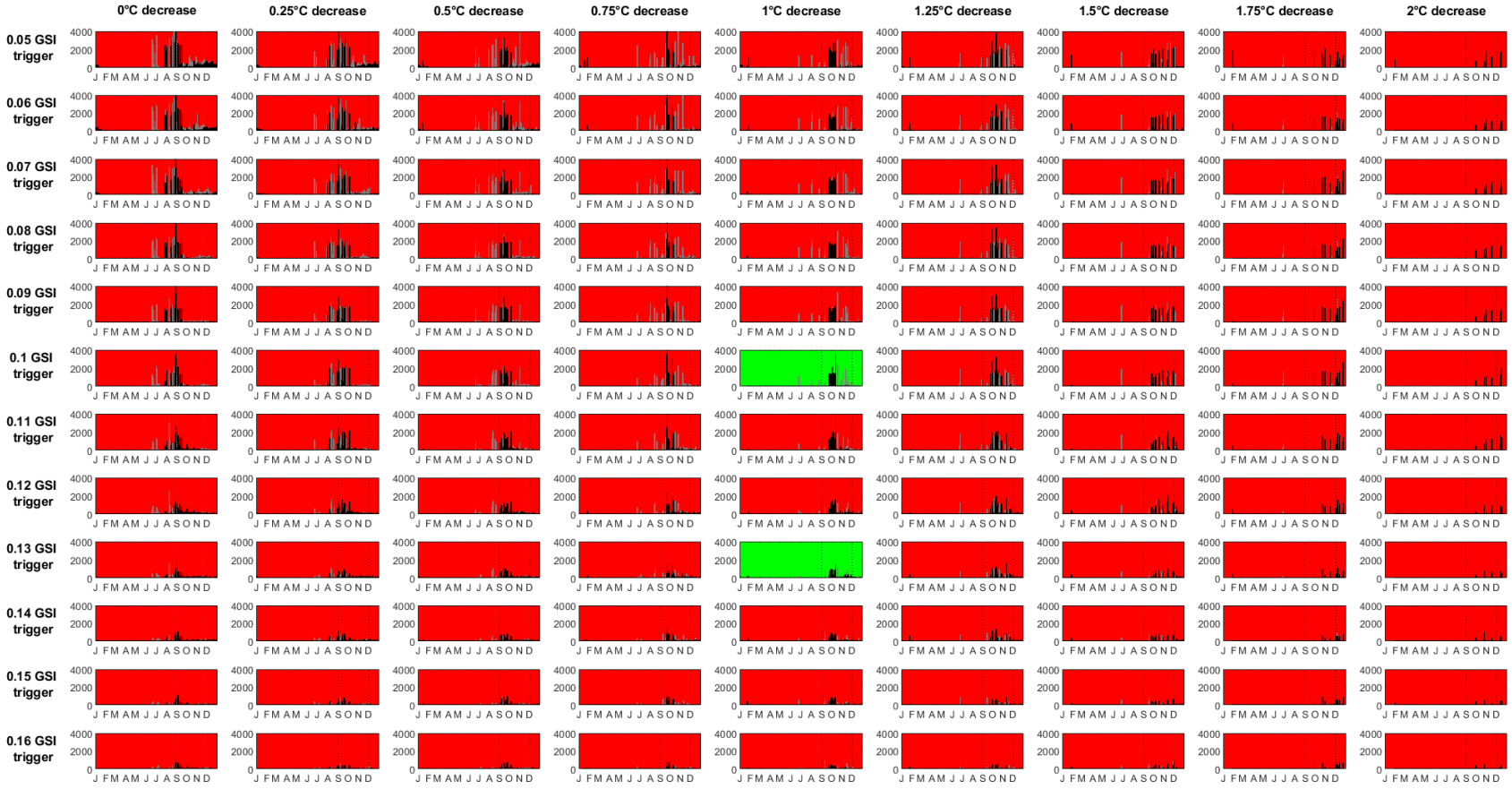

Sup. Mat. 3.2: Output of the model in terms of number of individuals of *Arenicola marina* spawning per day along the year (from January J to December D) in France (black bars) and Scotland (grey bars) with Sea-Surface Temperature decrease values from O°C to 2°C over two weeks and GSI (wet weight of gametes over total wet weight of the individual) trigger values between 0.05 and 0.16. Vertical dotted lines represent the main period of observation of spawning periods at both sites (De Cubber et al., 2018;Watson, 2000). Red backgrounds show that less than 80% of the spawning events are simulated within this period, green backgrounds show that more than 80% of the spawning events are simulated within this period.

Sup. Mat. 4 - Location, coordinates and authors referring to Arenicola marina *or* A. defodiens*'s occurrence used in this study.*

Num.	Location	Longitude	Latitude	Reference
*	Kandalashka Bay (Russia)	33.20126392	66.53614774	Pires et al. (2015)
1	Lindholmen (Sweden)	11.12555	58.8907333	Luttikhuizen and Dekker (2010)
*	Saltö (Sweden)	11.14779414	58.87222353	Luttikhuizen and Dekker (2010)
2	East Sands (St Andrews, Scotland)	-2.779435	56.338128	Watson and Bentley (1997)
3	Eden Estuary (St Andrews, Scotland)	-2.846838	56.363593	Watson and Bentley (1997)
4	Dunbar (Scotland)	-2.510515	56.002682	Watson and Bentley (1997)
5	Dorum-Neufeld (North Sea, Germany)	8.474212952	53.68955628	Schröer et al. (2009)
6	Slufter (Netherlands)	4.796710653	53.14159142	Luttikhuizen and Dekker (2010)
7	Eierlandse Gat (Wadden Sea, Netherlands)	4.971833333	53.1408833	Luttikhuizen and Dekker (2010)
8	Schorren (Wadden Sea, Netherlands)	4.90075	53.11675	Luttikhuizen and Dekker (2010)
9	Texel Beach (Netherlands)	4.764416667	53.1119167	Luttikhuizen and Dekker (2010)
10	Mok (Wadden Sea, Netherlands)	4.760394598	53.00706617	Luttikhuizen and Dekker (2010)
11	Molenrak (Netherlands)	4.695916667	53.0159167	Luttikhuizen and Dekker (2010)
12	Malzwin (Wadden Sea, Netherlands)	4.903133333	52.9819667	Luttikhuizen and Dekker (2010)
13	Huiduinen (Netherlands)	4.717333333	52.9479167	Luttikhuizen and Dekker (2010)
14	Pembrey (Wales)	-4.256619	51.67684	Cadman and Nelson-Smith (1993)
15	Whiteford (Gower, Wales)	-4.251745	51.641174	Cadman and Nelson-Smith (1993)
16	Jersey Marine (Wales)	-3.855282	51.614809	Cadman and Nelson-Smith (1993)
*	Terneuzen (Netherlands)	3.796070515	51.34671156	Luttikhuizen and Dekker (2010)
17	Wimereux (France)	1.604804899	50.76702711	De Cubber et al. (2018)
18	Le Touquet (France)	1.576889725	50.5217217	De Cubber et al. (2018)
19	Fort Mahon (France)	1.5483621	50.34030109	De Cubber et al. (2018)
20	Ault (France)	1.451783331	50.11079353	De Cubber et al. (2018)
21	Roscoff (France)	-3.987793196	48.72783611	Pires et al. (2015)
*	Arcachon (France)	-1.1606092	44.66448716	Pires et al. (2015)
22	San Sebastian (Spain)	-1.976031	43.327907	Pires et al. (2015)
23	Viana do Castelo (Portugal)	-8.833605	41.677859	Pires et al. (2015)
24	Porto (Portugal)	-8.679619	41.151247	Pires et al. (2015)
25	Setubal (Portugal)	-8.925142	38.474085	Pires et al. (2015)
26	Vila Nova de Milfontes (Portugal)	-8.805631	37.783829	Pires et al. (2015)
27	Alvor (Portugal)	-8.597985	37.121745	Pires et al. (2015)
28	Cadiz (Spain)	-6.288526	36.60041	Pires et al. (2015)

* These sites were not kept in the study due to the bad quality on the environmental data extracted there (see Sup. Mat. 2 for further details).

Sup. Mat. 5 - Model Stability

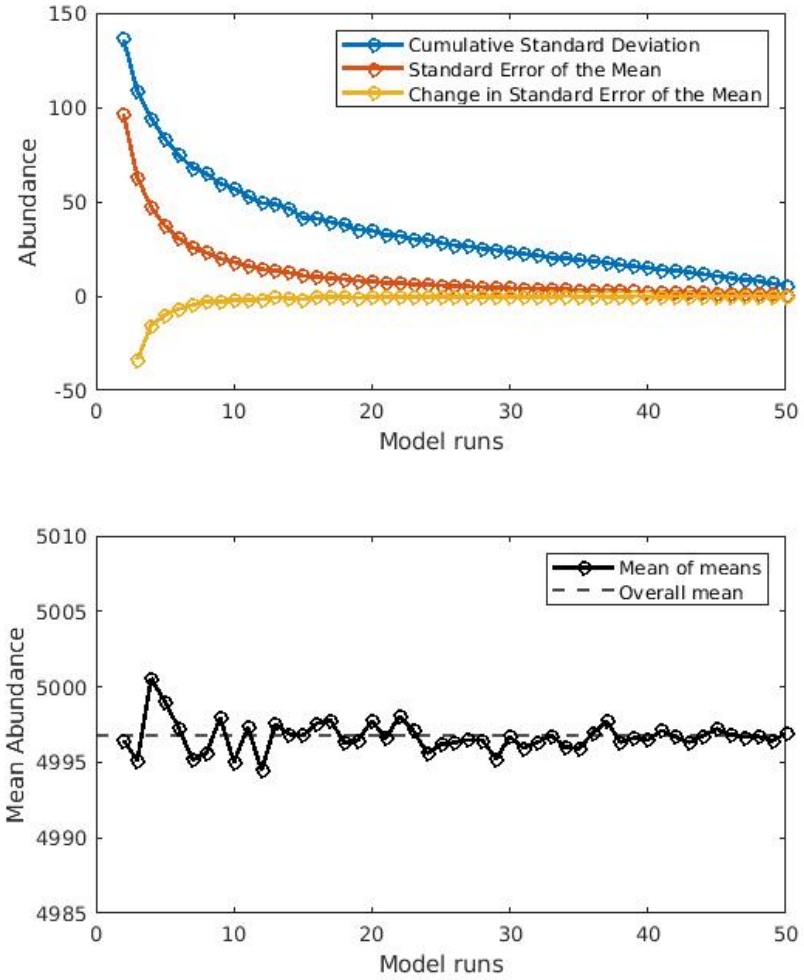

Evolution of standard deviation, standard error of the mean (SEM, with $SEM = \sigma/\sqrt{N}$) and $dSEM$ (top panel) and mean of means (bottom panel) according to the number of model runs chosen.

Sup. Mat. 6 - Mean values and associated of the biological traits at each sites and for each environmental scenario for the two species.

Sites and scenarios	*Arenicola marina*					*Arenicola defodiens*				
	Abundance	TSB	Lp,pop	Lmax,pop	TRO	Abundance	TSB	Lp,pop	Lmax,pop	TRO
1	6331 ± 154	46789 ± 1228	2.96 ± 0.005	10.76 ± 3.49	1.1 10^9 ± 1.6 10^9	378 ± 7	4912 ± 212	1.51 ± 0.003	12.34 ± 0.17	1.4 10^9 ± 6.7 10^8
2	5448 ± 186	37474 ± 2185	2.97 ± 0.003	11.31 ± 3.60	1.6 10^9 ± 2.4 10^9	0 ± 0	0 ± 0	0 ± 0	0 ± 0	0 ±1 0
3	6164 ± 275	37545 ± 1868	2.93 ± 0.003	9.33 ± 1.29	4.2 10^8 ± 6.1 10^8	393 ± 8	3506 ± 226	1.47 ± 0.001	7.86 ± 0.09	4.0 10^8 ± 1.5 10^8
4	4750 ± 132	11434 ± 460	2.96 ± 0.006	11.25 ± 3.31	1.5 10^9 ± 2.3 10^9	410 ± 4	1221 ± 23	1.50 ± 0	12.33 ± 0.16	1.7 10^9 ± 6.2 10^8
5	6659 ± 183	65607 ± 3496	2.96 ± 0.002	11.98 ± 3.09	1.6 10^9 ± 2.4 10^9	398 ± 6	13692 ± 234	1.51 ± 0	13.16 ± 0.17	2.1 10^9 ± 6.7 10^8
6	5702 ± 155	19144 ± 654	2.93 ± 0.005	9.10 ± 1.53	4.2 10^8 ± 6.1 10^8	410 ± 6	2483 ± 75	1.48 ± 0.001	8.09 ± 0.12	4.5 10^8 ± 1.6 10^8
7	6604 ± 198	56704 ± 3604	2.96 ± 0.004	11.04 ± 2.67	1.0 10^9 ± 1.5 10^9	398 ± 5	11411 ± 319	1.51 ± 0.001	11.60 ± 0.18	7.4 10^8 ± 4.3 10^7
8	6693 ± 104	65233 ± 2108	2.96 ± 0.003	10.78 ± 2.42	9.6 10^8 ± 1.4 10^9	399 ± 3	14764 ± 433	1.50 ± 0.001	10.65 ± 0.13	1.1 10^9 ± 4.3 10^8
9	5679 ± 205	19652 ± 706	2.96 ± 0.003	11.18 ± 3.72	1.6 10^9 ± 2.5 10^9	407 ± 6	2697 ± 75	1.51 ± 0.001	13.29 ± 0.09	2.2 10^9 ± 7.3 10^8
10	6225 ± 151	39989 ± 1624	2.96 ± 0.004	10.72 ± 3.17	1.2 10^9 ± 1.9 10^9	401 ± 8	6978 ± 109	1.51 ± 0.001	11.72 ± 0.14	1.4 10^8 ± 4.7 10^8
11	5936 ± 144	38816 ± 1653	2.95 ± 0.003	11.32 ± 1.97	7.3 10^8 ± 1.1 10^9	0 ± 0	0 ± 0	0 ± 0	0 ± 0	0 ± 0
12	6788 ± 169	67794 ± 2868	2.93 ± 0.057	10.13 ± 3.61	7.9 10^8 ± 1.2 10^9	402 ± 5	15046 ± 430	1.51 ± 0.004	6.72 ± 0.29	5.5 10^6 ± 6.0 10^5
13	6619 ± 188	52510 ± 1859	2.91 ± 0.003	9.06 ± 0.82	2.3 10^8 ± 3.1 10^8	395 ± 5	9233 ± 239	1.46 ± 0.001	6.58 ± 0.17	2.1 10^8 ± 5.9 10^7
14	6020 ± 219	31853 ± 1405	2.95 ± 0.004	10.47 ± 1.93	7.4 10^8 ± 1.1 10^9	410 ± 4	4795 ± 221	1.49 ± 0.002	9.35 ± 0.11	7.6 10^8± 3.0 10^8
15	6280 ± 132	42238 ± 1552	2.95 ± 0.004	10.47 ± 2.76	9.7 10^8 ± 1.5 10^9	400 ± 9	6228 ± 258	1.50 ± 0.001	10.13 ± 0.10	1.0 10^9 ± 3.9 10^8
16	6210 ± 167	33438 ± 1453	2.94 ± 0.002	10.38 ± 1.99	7.3 10^8 ± 1.1 10^9	408 ± 9	5516 ± 109	1.48 ± 0.001	9.62 ± 0.14	7.9 10^8 ± 3.5 10^8
17	5376 ± 125	16401 ± 629	2.92 ± 0.005	9.24 ± 1.12	3.7 10^8 ± 5.3 10^8	411 ± 6	2273 ± 35	1.47 ± 0.002	7.26 ± 0.07	3.5 10^8 ± 1.2 10^8
18	5819 ± 193	27023 ± 1117	2.95 ± 0.006	10.00 ± 1.97	6.6 10^8 ± 9.9 10^8	412 ± 3	2792 ± 64	1.49 ± 0.002	8.33 ± 0.22	5.6 10^8 ± 2.0 10^8
19	6140 ± 172	40394 ± 2003	2.96 ± 0.003	10.82 ± 2.41	1.1 10^9 ± 1.6 10^9	402 ± 6	5242 ± 108	1.50 ± 0.001	10.07 ± 0.13	1.0 10^9 ± 3.7 10^8
20	6183 ± 165	35094 ± 1731	2.97 ± 0.006	10.04 ± 2.23	9.1 10^8 ± 1.4 10^9	404 ± 7	4018 ± 143	1.50 ± 0.001	9.27 ± 0.21	8.7 10^8 ± 2.6 10^8
21	172 ± 51	44 ± 14	2.71 ± 0.009	4.12 ± 0.10	3.8 10^6 ± 9.0 10^5	403 ± 27	47 ± 7	1.32 ± 0.002	2.37 ± 0.04	9.6 10^7± 1.7 10^6
22	97 ± 50	10 ± 6	2.56 ± 0.038	3.33 ± 0.10	2.1 10^6 ± 8.0 10^5	0 ± 0	0 ± 0	0 ± 0	0 ± 0	0 ± 0
23	4885 ± 144	10382 ± 388	2.92 ± 0.006	8.58 ± 0.65	2.8 10^8 ± 3.9 10^8	409 ± 4	430 ± 46	1.47 ± 0.002	5.87 ± 0.21	1.2 10^8 ± 5.4 10^7
24	5815 ± 205	19082 ± 1156	2.93 ± 0.004	9.38 ± 1.08	5.1 10^8 ± 7.4 10^8	409 ± 6	1513 ± 135	1.47 ± 0.003	6.89 ± 0.15	2.5 10^8 ± 1.8 10^8
25	137 ± 69	24 ± 12	2.81 ± 0.018	3.69 ± 0.18	5.4 10^6 ± 1.0 10^6	0 ± 0	0 ± 0	0 ± 0	0 ± 0	0 ± 0
26	150 ± 76	29 ± 16	2.68 ± 0.024	3.94 ± 0.16	6.0 10^6 ± 2.1 10^6	1 ± 1	0 ± 0	1.38 ± 0.001	1.68 ± 0.5	2.0 10^5 ± 1.3 10^5
27	951 ± 185	295 ± 66	2.83 ± 0.009	4.98 ± 0.17	3.2 10^7 ± 4.0 10^6	0 ± 0	0 ± 0	0 ± 0	0 ± 0	0 ± 0
28	2233 ± 108	1250 ± 162	2.84 ± 0.008	5.67 ± 0.18	5.2 10^7 ± 3.5 10^7	0 ± 0	0 ± 0	0 ± 0	0 ± 0	0 ± 0
SST∼10 & chl-a∼1	93 ± 51	23 ± 14	2.72 ± 0.012	4.04 ± 0.13	2.6 10^6± 7.0 10^5	369 ± 80	15 ± 4	1.34 ± 0.002	2.50 ± 0.05	9.1 10^6 ± 2.6 10^6
SST∼12 & chl-a∼1	135 ± 80	34 ± 22	2.71 ± 0.012	4.07 ± 0.17	3.6 10^6± 1.6 10^6	388 ± 84	15 ± 3	1.33 ± 0.004	2.37 ± 0.04	9.6 10^6 ± 2.4 10^6
SST∼19 & chl-a∼1	214 ± 83	57 ± 23	2.70 ± 0.012	4.25 ± 0.12	5.7 10^6± 1.2 10^6	375 ± 59	14 ± 2	1.32 ± 0.005	2.25 ± 0.04	5.1 10^6 ± 1.2 10^6
SST∼10 & chl-a∼5	5620 ± 140	28351 ± 1217	2.94 ± 0.004	10.78 ± 1.68	5.5 10^8 ± 8.1 10^8	409 ± 5	1039 ± 33	1.49 ± 0.001	9.71 ± 0.09	6.7 10^8 ± 2.3 10^8
SST∼12 & chl-a∼5	5576 ± 193	30672 ± 1747	2.95 ± 0.004	10.66 ± 1.93	6.9 10^8± 1.0 10^9	409 ± 7	953 ± 45	1.49 ± 0.001	9.31± 0.11	7.5 10^8 ± 2.9 10^8
SST∼19 & chl-a∼5	5702 ± 245	35808 ± 1955	2.96 ± 0.003	11.27 ± 1.70	1.0 10^9 ± 1.5 10^9	407 ± 5	968 ± 17	1.50 ± 0.002	9.43 ± 0.16	1.2 10^9 ± 3.9 10^8
SST∼10 & chl-a∼14	6015 ± 172	47344 ± 2276	2.96 ± 0.008	10.97 ± 3.28	1.0 10^9 ± 1.5 10^9	383 ± 11	971 ± 35	1.50 ± 0.004	11.91 ± 0.19	1.2 10^9± 6.0 10^8
SST∼12 & chl-a∼14	6003 ± 213	50906 ± 2460	2.96 ± 0.007	10.39 ± 4.09	1.2 10^9 ± 1.9 10^9	371 ± 12	949 ± 33	1.50 ± 0.002	12.17 ± 0.20	1.3 10^9± 5.4 10^8
SST∼19 & chl-a∼14	5943 ± 83	59212 ± 1844	2.97 ± 0.003	11.67 ± 3.90	2.7 10^9 ± 2.7 10^9	349 ± 13	1115 ± 36	1.50 ± 0.002	13.00 ± 0.13	1.4 10^9 ± 3.5 10^8

Sup. Mat. 7.1 - Interpolated time-series of Sea-Surface Temperature (K) at each study site (see Sup. Mat. 1 for correspondence between numbers and sites) used further in the DEB-IBM for Arenicola marina *and* A. defodiens. *Sites are ordered from the higher latitudes to the lower latitudes.*

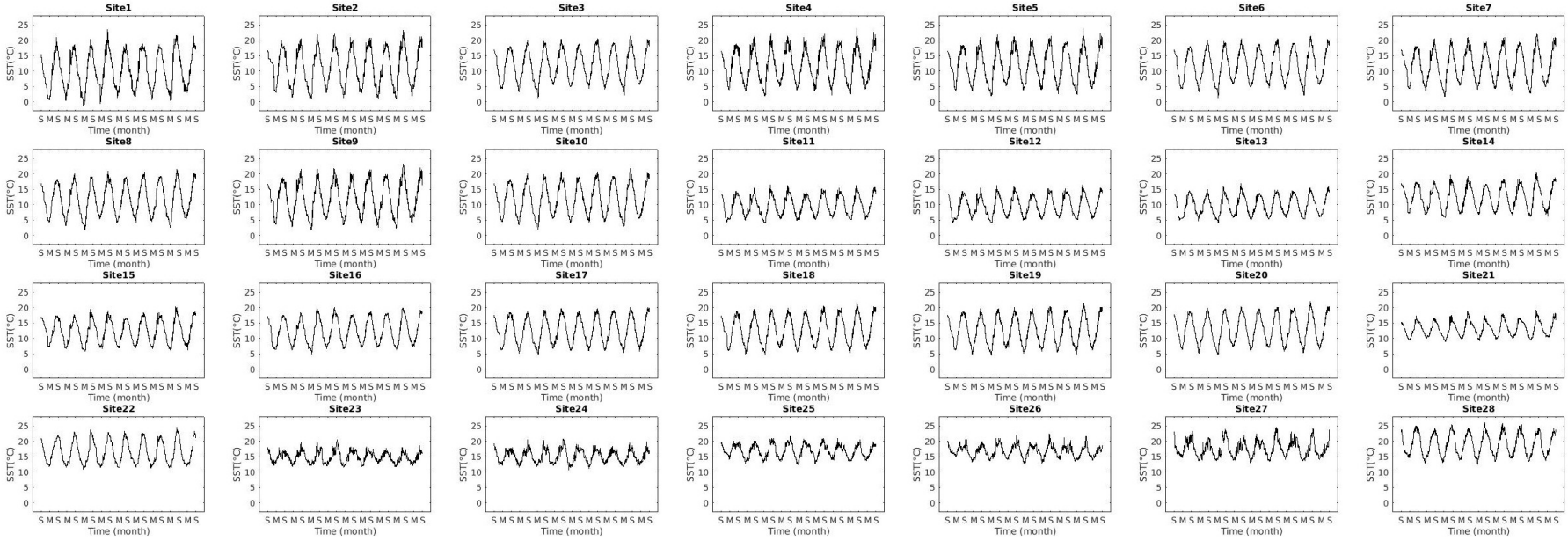

Sup. Mat. 7.2 - Interpolated time-series of chlorophyll-a concentrations ($\mu g.L^{-1}$) at each study site (see Sup. Mat. 1 for correspondence between numbers and sites) used further in the DEB-IBM for Arenicola marina *and* A. defodiens. *Sites are ordered from the higher latitudes to the lower latitudes.*

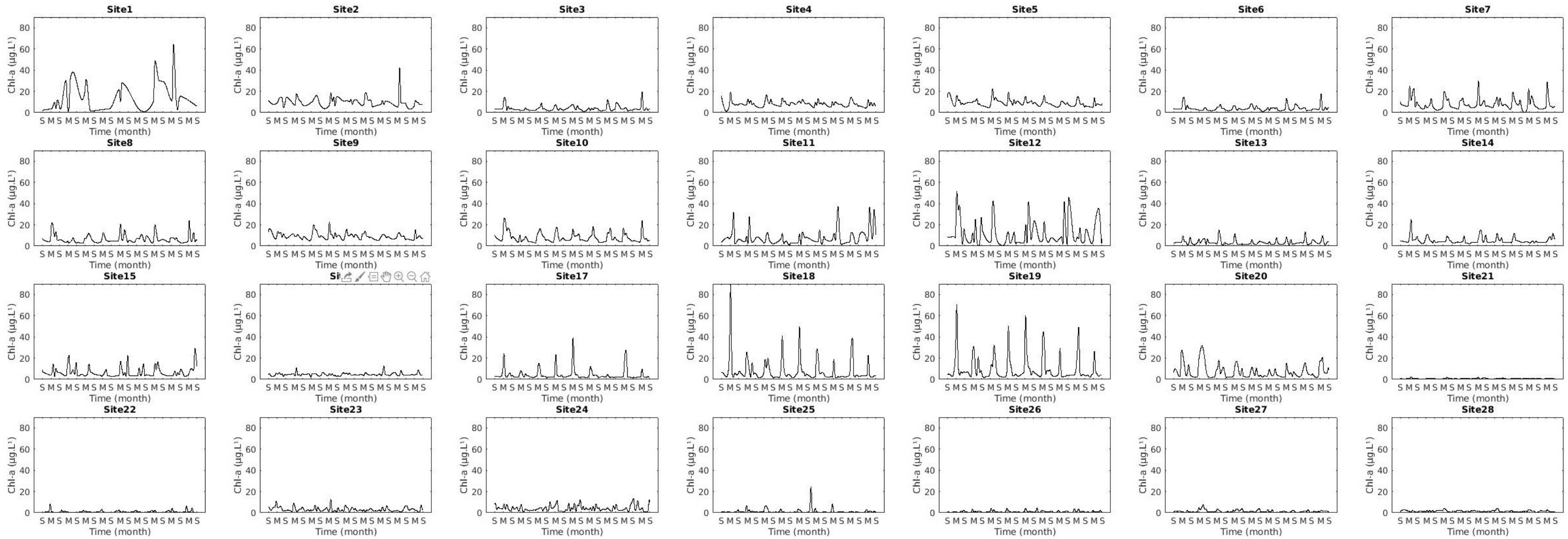

Sup. Mat. 8 - A. defodiens*' simulated abundance and associated chl-a and SST according to time (d) over the two cycles of 10 years at the 6 sites where populations were predicted to crash. Site numbers refer to Sup. Mat. 1.*